THE HAWAII GEOTHERMAL PROJECT

A PARAMETRIC STUDY OF A VERTICAL HEAT EXCHANGER DESIGNED FOR GEOTHERMAL POWER PLANT APPLICATION

TECHNICAL REPORT No. 5

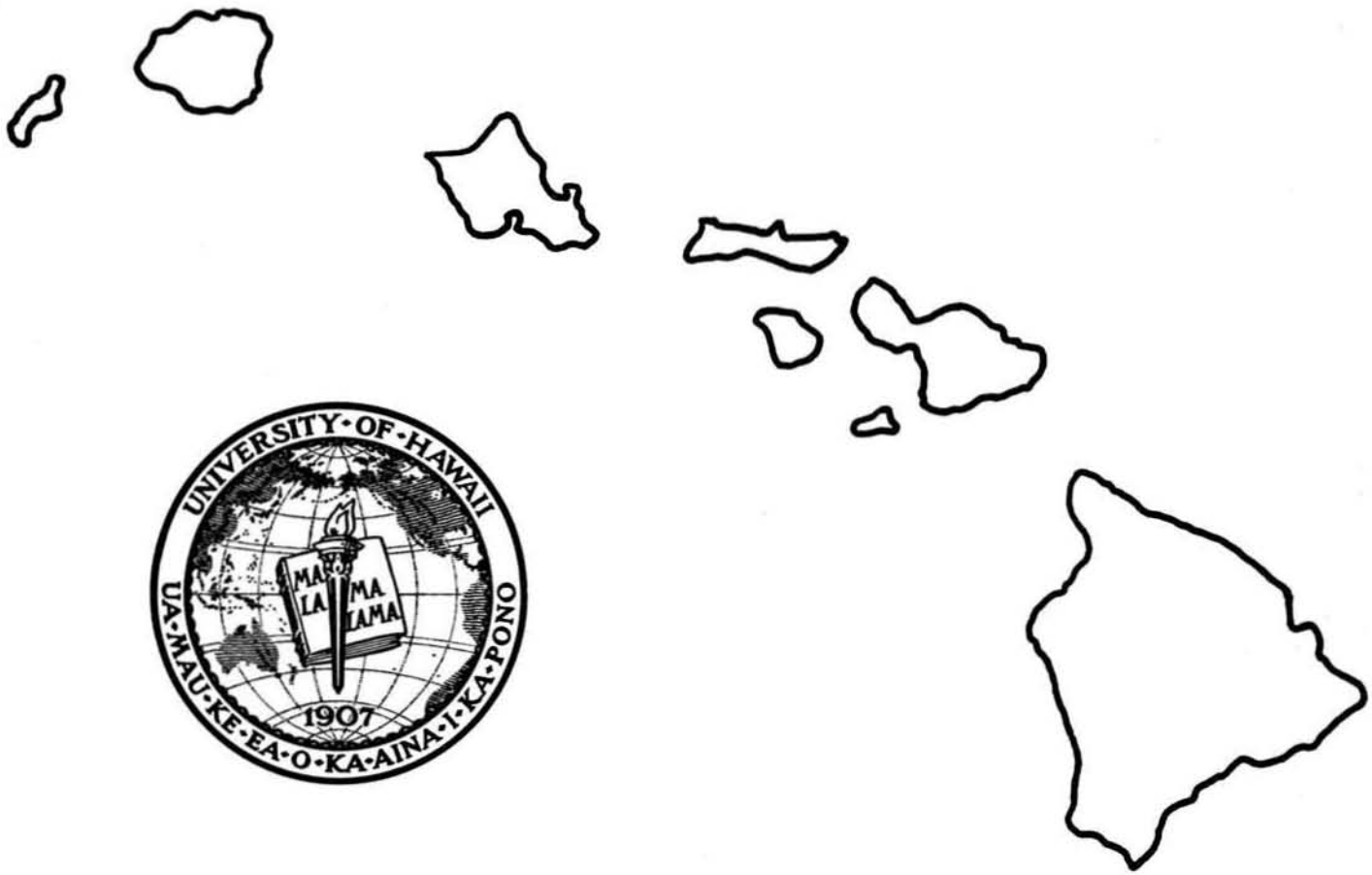

HAWAII GEOTHERMAL PROJECT

ENGINEERING PROGRAM

A PARAMETRIC STUDY OF A VERTICAL HEAT EXCHANGER DESIGNED FOR GEOTHERMAL POWER PLANT APPLICATION

TECHNICAL REPORT No. 5

September 16, 1974

Prepared Under

NATIONAL SCIENCE FOUNDATION

RESEARCH GRANT NO. GI-38319

By

Gary Shimozono

Hi Chang Chai

Deane Kihara

College of Engineering
University of Hawaii
Honolulu, Hawaii 96822

TABLE OF CONTENTS

ABSTRACT

The preliminary design of a vertical, counterflow, shell and tube heat exchanger for use in a binary fluid power cycle is presented. The heat exchanger is to be part of a representative geothermal power plant generating 10 MW utilizing geothermal brine at 350°F with isobutane as the working fluid.

The computational procedure for determining heat transfer coefficients, tube lengths, number of tubes, and pressure drops is outlined. Detailed in graphical form are results of a parametric study showing how these four parameters are affected by changes in turbine inlet temperature, tube diameter, tube pitch, isobutane velocity, scale thickness, pinch point temperature difference, and system pressure.

LIST OF SYMBOLS

Notation		
A	Area	ft^2
C	Specific heat at constant pressure	Btu/lbm-°F
D	Tube diameter	in
De	Equivalent diameter	in
f	Friction factor	---
g_c	Gravitational constant	lbm-ft/lbf-sec^2
G	Mass velocity	lbm/hr-ft^2
h	Enthalpy	Btu/lbm
H	Heat transfer coefficient	Btu/hr-ft^2-°F
k	Thermal conductivity	Btu/hr-ft-°F
L	Tube length	ft
$\dot{m}$	Mass flow rate	lbm/hr
P	Pressure	lbf/ft^2
Q	Heat flux per tube	Btu/hr
s	Suppression factor	---
S	Distance between centerlines of adjacent tubes	in
Sc	Scale thickness	in
T	Temperature	°F
U	Conductance	Btu/hr-ft^2-°F
V	Velocity	ft/sec
x	Vapor quality	---

Greek Letters

ΔT	Wall superheat	F
ΔP	Difference in vapor pressure corresponding to ΔT	psi
λ	Latent heat of vaporization	Btu/lbm
μ	Viscosity	lbm/hr-ft
ρ	Density	lbm/ft^3
σ	Surface tension	lbf/ft^2
γ	Specific weight	lbf/ft^3
ϕ	Two-phase frictional multiplier	---
θ	Angle between tube axis and direction of gravity	degrees

Dimensionless Groups

Nu	Nusselt number	$[\frac{HD}{k}]$
Pr	Prandtl number	$[\frac{\mu C}{k}]$
Re	Reynolds number	$[\frac{GD}{\mu}]$
X_{tt}	Martinelli parameter	$\left[\frac{x}{1-x}\right]^{0.9}\left[\frac{\rho_L}{\rho_v}\right]^{0.5}\left[\frac{\mu_v}{\mu_L}\right]^{0.1}$

Subscripts

B	Brine
mac	Macroscopic
mic	Microscopic
L	Liquid
Sc	Scale
SF	Secondary Fluid
v	Vapor condition
w	Wall condition
o	Outside (tube diameter)
i	Inside (tube diameter)

LIST OF FIGURES

INTRODUCTION

Although motive power generation from a low temperature source using a secondary fluid has been limited to a few applications thus far [1, 2], more extensive use of such systems is being planned in order to utilize the energy available in low temperature geothermal fields [3, 4].

Heat exchangers will be at the interface between the geothermal fluid and the secondary fluid and will constitute an essential part of this particular means of energy conversion. The design of the primary heat exchanger will depend on parameters of the power producing cycle as well as on the properties of the geothermal fluid.

This report is concerned with the effects of various parameters on the design of a heat exchanger to be used in a geothermal power cycle using a secondary fluid and is intended to be a first step in a program to arrive at an optimum design. Figure 1 is a schematic of the heat exchanger and the Rankine cycle using a secondary fluid.

The heat exchanger to be studied is for a representative geothermal power plant of 10 MW capacity utilizing liquid brine at 350°F. The secondary fluid is isobutane, the substance selected by both Holt et al. [3] and Anderson [4].

Required for this study were sufficiently detailed correlations for convective boiling heat transfer in tube bundles which could be used without the introduction of artificial correction factors. Unfortunately, such correlations are highly proprietary in nature and were not available. However, correlations were found in the open literature for tubular flow [5, 6, 7, 8]. Since it is possible to treat the flow channels in a vertical shell and tube heat exchanger as annular tubes of some equivalent diameter, a vertical, counterflow, shell and tube heat exchanger was selected for this study. The arrangement of the tubes and the equivalent annular flow area are shown in Figure 2. Brine flows down through the tubes while the secondary fluid flows up on the shell side. A typical heat exchanger using this configuration is shown in Figure 3.

COMPUTATIONAL PROCEDURE

Mass Flow Rates

A preliminary study was conducted [9] of the simple Rankine cycle using isobutane for the following conditions:

Power output	10 MW
Heat source	Liquid brine at 350°F
Turbine inlet pressure	400 psia
Condenser outlet conditions	Saturated liquid at 100°F
Turbine efficiency	85%
Pump efficiency	75%
Pressure losses and heat losses neglected	

The resultant curves for the isobutane and brine flow rates required are shown in Figure 4. It is to be noted that a minimum exists in the brine flow rate curve for a turbine inlet temperature of 280°F.

The relationship between the temperatures of brine and isobutane at 400 psia is shown in Figure 5. For isobutane exit temperatures between 245°F and 330°F, the pinch point occurs at station 3.

Temperature Differences

The log mean temperature of any section is obtained through the use of the following equation:

$$T_{mean} = \frac{T_1 - T_2}{\ln\left(\frac{T_1}{T_2}\right)} \qquad (1)$$

To determine the log mean temperature difference of a section, the log mean temperatures of the brine and secondary fluid are computed and a difference is taken between the mean temperatures.

Heat Transfer Coefficients

In computing the shell side heat transfer coefficients, an equivalent diameter for the flow channel was calculated and used in Nusselt number expressions originally intended for circular tubes. In the single-phase sections, equations suggested by Kays [10] for fully developed turbulent flow in circular tubes were used. For the liquid-phase sections, the following equation was recommended:

$$Nu = 0.0155\ Pr^{0.5}\ Re^{0.83} \tag{2}$$

The equation recommended for the vapor-phase section was

$$Nu = 0.021\ Pr^{0.6}\ Re^{0.8} \tag{3}$$

Since the brine never departs from a liquid-phase, the tube side heat transfer coefficients were calculated from the same equation used for the liquid-phase portions on the shell side.

In the region where boiling occurs, the correlation presented by Chen [5] was used. He postulated that two mechanisms contributed to the heat transfer process during convective boiling of a saturated liquid. The first mechanism is a macroconvective mechanism which normally operates with flowing fluids. The second mechanism is a microconvective mechanism which is associated with bubble nucleation and growth. As in other similar studies, it is postulated that the two mechanisms are additive in their contribution to the total heat transfer.

For the macroconvective contribution, it was postulated that the heat transfer coefficient could be determined from a modified form of the Dittus-Boelter equation. Chen suggested the following equation:

$$H_{mac} = 0.023\ Re_L^{0.8}\ Pr_L^{0.4}\ \frac{k_L}{D}\ F(X_{tt}) \tag{4}$$

where F is the ratio of the two-phase Reynolds number to the liquid Reynolds number based on the liquid fraction of the flow. The ratio F was assumed to be a function of the Martinelli parameter, X_{tt}, which is a two-phase flow modulus. This assumption was based on the observation that F is strictly a

flow parameter and analogous to momentum transfer in two-phase flow for which the Martinelli parameter is used. Experimental data confirmed the assumption and showed the actual dependence of F on the Martinelli parameter. The ratio F was found to increase with increasing values of the reciprocal Martinelli parameter, indicating the existence of a direct relationship between the turbulence associated with two-phase flow and vapor fraction.

Chen used the analysis of Forster and Zuber [11] as the basis for his formulation of the microconvective contribution to heat transfer. For the microconvective component, Chen suggested the following equation:

$$H_{mic} = 0.00122 \frac{k_L^{0.79} C_L^{0.45} \rho_L^{0.49} g_c^{0.25}}{\sigma^{0.5} \mu_L^{0.29} \lambda^{0.24} \rho_V^{0.24}} \Delta T^{0.24} \Delta P^{0.75} s \quad (5)$$

where s is the ratio of the effective superheat to the total superheat of the wall. The suppression factor, s, approaches unity at zero flow rate and zero at infinite flow rate. It was postulated, then experimentally verified, that s could be expressed as a function of the local two-phase Reynolds number. In Equation (5), ΔT represents the difference between wall temperature and the saturation temperature of the fluid. ΔP is the difference in vapor pressure corresponding to ΔT.

The expression for the total heat transfer coefficient is simply

$$H_{total} = H_{mic} + H_{mac} \quad (6)$$

Boiling coefficients were calculated for a quality of 50% from Equation (6). This quality was used because it represents the average quality of the entire boiling section. However, Chen's equation requires knowledge of the heat transfer area of the boiling section. This requirement compels the use of an iterative technique to determine the heat transfer coefficient and its corresponding heat transfer area. In the discussion on tube length determination, the procedure for determining boiling coefficients will be elaborated.

Tube Length

To determine the tube length needed to transfer the required amount of heat from the brine to the secondary fluid, the flow was divided into three regions: the non-boiling, boiling, and superheated regions. The procedure used in the two single-phase regions was essentially the same.

The required heat transfer from each tube was computed from the mass flow rate and the inlet and outlet conditions of the secondary fluid for each region; symbolically,

$$Q = \dot{m}_{SF} \left(\frac{h_{SF,in} - h_{SF,out}}{\text{No. of Tubes}} \right) \tag{7}$$

From heat transfer considerations,

$$Q = \frac{T_{B,mean} - T_{SF,mean}}{\frac{1}{L}\left[\frac{1}{\pi H_B D_i} + \frac{\ln\left(\frac{D_i}{D_i - 2Sc}\right)}{2\pi k_{Sc}} + \frac{\ln\left(\frac{D_o}{D_i}\right)}{2\pi k_w} + \frac{1}{\pi H_{SF} D_o} \right]} \tag{8}$$

Equating Equations (7) and (8) and rearranging, gives an expression for tube length.

$$L = \frac{\dot{m}_{SF}(h_{SF,in} - h_{SF,out})}{\text{No. of Tubes}} \frac{\left[\frac{1}{\pi H_B D_i} + \frac{\ln\left(\frac{D_i}{D_i - 2Sc}\right)}{2\pi k_{Sc}} + \frac{\ln\left(\frac{D_o}{D_i}\right)}{2\pi k_w} + \frac{1}{\pi H_{SF} D_o} \right]}{T_{B,mean} - T_{SF,mean}} \tag{9}$$

In the above equations, D_i, D_o, Sc, and w denote inside diameter, outside diameter, scale thickness and reference to tube wall conditions, respectively.

These equations are applicable to conditions where the heat transfer coefficients are independent of heat transfer area. As mentioned earlier, this condition does not exist in the boiling region where the boiling

coefficient is indeterminable without knowledge of the heat transfer area. This would seem to prohibit the use of Equation (9) for determining tube lengths associated with the boiling region. It is possible, however, to use an iterative technique in which tube lengths are assumed, and, using Equation (9) in conjunction with other heat transfer equations, the tube length for the boiling region can be found.

With the assumption of a tube length, the following equation allows the determination of the outside surface temperature of the tube:

$$T_{SF,w} = T_{B,w} - Q \left[\frac{\ln\left(\frac{D_i}{D_i - 2Sc}\right)}{2\pi L k_{Sc}} + \frac{\ln\left(\frac{D_o}{D_i}\right)}{2\pi L k_w} \right] \tag{10}$$

The surface temperature obtained from the preceding equation is used to determine the boiling coefficient of the secondary fluid, which upon substitution into Equation (9) yields a tube length. A comparison is then made between the assumed and computed tube lengths. If the lengths are equal, then the tube length which corresponds to the conditions of the section in question has been found. If there should be a discrepancy between the lengths, then another length is assumed and the procedure is repeated. A flowchart of this procedure can be seen in Figure 6.

Pressure Drop

In the heat transfer analysis, the flow channels for the secondary fluid were treated as tubes of some equivalent diameter. This treatment of the flow channels was continued in the pressure drop analysis and relations developed for pipe flow were employed in determining pressure drops.

Pressure drop in pipe flow is comprised of three components: frictional, gravitational, and accelerational. Preliminary computations showed that accelerational pressure drops were negligible in comparison to the frictional and gravitational components. Therefore, discussion will be limited to frictional and gravitational pressure drops.

Single-phase frictional pressure drops are determined with the aid of friction coefficients associated with the flow conditions under consideration. The friction coefficient, when multiplied by $(\gamma LV^2/2g_c)(L/D)$, results in the

frictional pressure drop of the section. In determining the friction coefficient, a functional representation of the Moody diagram was used. The relation used is known as the Colebrook equation [12] and is shown below.

$$
\begin{aligned}
f &= a + bRe^{-c} \\
a &= 0.094k^{0.225} + 0.53k \\
b &= 88k^{0.44} \\
c &= 1.62k^{0.134} \\
k &= \varepsilon/D
\end{aligned}
\tag{11}
$$

f is the friction factor. In the Colebrook equation, ε denotes the surface roughness of the tube through which the fluid is flowing. In performing the actual friction coefficient computations, it was necessary to assume a surface roughness for the flow channel since no specific type of tube was being considered. The assumed value of ε was .00015 feet.

Determining two-phase frictional pressure drops involved the use of a multiplier, ϕ, which when multiplied with a pressure drop determined from single-phase relations, results in the two-phase pressure drop. An expression suggested by Wallis [13] for one-dimensional two-phase turbulent flow was employed to ascertain the values of the two-phase multipliers. In developing the expression for the multiplier, Wallis used a homogeneous equilibrium flow model in which the average values of velocity, temperature, and chemical potential are the same for each component. In the procedure suggested by Wallis, a liquid viscosity is used in the Reynolds number computation. The computed Reynolds number is then used to find a single-phase pressure drop in a manner similar to that described earlier. The pressure drop multiplier is given by

$$
\phi = \left[1 + x\left\{\frac{\rho_L}{\rho_V} - 1\right\}\right]\left[1 + x\left\{\frac{\mu_L}{\mu_V} - 1\right\}\right]^{-1/4} \tag{12}
$$

Since the quality in the boiling section varies from 0 to 100%, an average quality of 50% was used to determine the pressure drop multiplier for the whole section.

Gravitational pressure drop was the major contributor to the total pressure drop, and its contribution was calculated from the following expression:

$$\Delta P = \rho_{mean} g \cos \theta \tag{13}$$

where ρ_{mean} denotes mean density and θ is the angle between the tube axis and the direction of gravity. The mean density of the boiling section was obtained from the expression:

$$\frac{1}{\rho_{mean}} = \frac{x}{\rho_v} + \frac{1 - x}{\rho_L} \tag{14}$$

In the actual computations, the flow was divided into the three major sections, and the mean density and length of each section was used to compute the gravitational and frictional pressure drop of each section. The pressure drops for each section were them summed to give the total pressure drop of the heat exchanger.

DISCUSSION OF RESULTS

Parameter values

The results contained in this section were obtained using a computer program whose primary function was to compute tube lengths and pressure drops for various input parameters. By varying the values of a particular input parameter, the effect of that parameter on tube length and pressure drop of a "standard heat exchanger" could be determined from the computer results.

The values which make up the standard set of parameters are listed below:

System pressure	400 psia
Turbine inlet temperature (isobutane exit temperature)	280°F
Tube diameter	1.0 inch
Tube material	Aluminum
Pitch	1.1
Brine inlet temperature	350°F
Scale thickness	0 inch
Isobutane velocity	7 feet per second
Pinch point temperature difference	20°F

In utilizing the computer program, all parameters except one are assigned the above values. The parameter of interest is then allowed to vary through a

range to determine the effect of such variation on the other parameters. The following is a list of the parameters and their corresponding input values:

Parameter	Input Values
System pressure	400, 600 psia
Turbine inlet temperature	245, 260, 280, 300, 320 °F
Tube diameter	1.0, 1.5, 2.0 inch
Pitch	1.1, 1.25, 1.5
Scale thickness	0, 0.01, 0.075, 0.10 inch
Isobutane velocity	4, 7, 10, 15 fps
Pinch point temperature difference	10, 15, 20, 25 °F

Effect of Turbine Inlet Temperature

Varying the turbine inlet temperature affects the design of the heat exchanger in several ways. One of the more significant effects involves changes in cycle efficiency which result in alterations of the mass flow rate of the working fluid. (See Figure 4). Another effect involves the outlet condition of the brine which changes as the turbine inlet temperature changes. Together these effects necessitate changes in heat exchanger design as turbine inlet conditions change.

The effect of the turbine inlet temperature on tube lengths can be seen in Figure 7. The tube lengths associated with the boiling and superheat sections are seen to increase as the turbine inlet temperature increases. The tube lengths associated with the non-boiling section show an inverse relationship with turbine inlet temperature and decrease in length as the turbine inlet temperature increases.

The relationship which exists between tube lengths of the various sections and turbine inlet temperature would not be expected from an inspection of the heat transfer coefficients alone. Figure 8 shows the isobutane heat transfer coefficients of the different sections as a function of turbine inlet temperature. Heat transfer coefficients are seen to remain constant in the non-boiling section, decrease in the boiling section and increase in the superheat section, as turbine inlet temperature increases. Brine heat transfer coefficients, shown in Figure 9, are seen to have a direct relationship to turbine inlet temperature. The

heat transfer coefficient behavior would seem to suggest tube length behavior other than that which is seen in Figure 7. However, a more significant factor becomes apparent when brine temperatures are examined.

Figure 10 is a temperature-enthalpy diagram which shows the effect of turbine inlet temperature on brine temperatures. To the right of the pinch point the temperature difference between brine and isobutane decreases as the turbine inlet temperature increases, while temperature difference to the left of the pinch point increases. This change in the temperature difference has the effect of changing the rate of heat transferred between the two fluids.

The heat flux associated with the tubes determines the necessary tube length and, as can be seen in Equation (15), it is directly proportional to the conductance and temperature difference between the fluids.

$$Q = UA\ (T_B - T_{SF}) \tag{15}$$

In general, heat transfer coefficients increase as turbine inlet temperature increases, with the exception of the shell side boiling coefficient which decreases. Therefore, the conductance between the brine and isobutane will increase along with the turbine inlet temperature. However, the changes in the temperature difference are significantly larger than those of the conductance. Consequently, temperature difference dictates the tube length relation with turbine inlet temperature.

From the discussion above, it can be ascertained that the turbine inlet temperature is a highly influential factor in heat exchanger design. It has been shown that a relation exists between heat transfer coefficients and turbine inlet temperature. The relationship, however, is not the same for all sections.

The increase in shell side heat transfer coefficient is seen to be very small for the superheat section and can be attributed to changes in the transport properties resulting from the increasing mean temperature of the section. It has been shown that heat transfer coefficients associated with single phase forced convection flow are functions of the Reynolds and Prandtl numbers. The expressions for Reynolds number, Re, and Prandtl number, Pr, are given below.

$$Re = \frac{G\ De}{\mu} \tag{16}$$

where $G = \rho V$

$$Pr = \frac{\mu C}{k} \tag{17}$$

An examination of the Reynolds number expression reveals that any effect attributable to increased velocity is negated by the decrease in density. Therefore, transport properties alone affect the heat transfer coefficients in this section.

In the boiling section, reductions in shell side heat transfer coefficients are experienced as turbine inlet temperature is increased. Boiling heat transfer coefficients have been shown to be a function of wall temperature, or more specifically, the amount by which the wall temperature exceeds the saturation temperature of the evaporating fluid. Previously it was noted that the brine temperature in the boiling section decreased with increasing turbine inlet temperature. Reductions in brine temperature causes corresponding reductions in shell side wall temperatures and the associated boiling heat transfer coefficients.

The shell side heat transfer coefficient in the non-boiling section is seen to be constant over the entire range of turbine inlet temperature. This was done intentionally by keeping the flow conditions fixed for each flow channel for all turbine inlet temperatures. This procedure was adopted in an effort to define flow conditions at a particular location and thus provide a basis for determining tube number, knowledge of which is essential for a heat transfer analysis.

From Figure 2, it can be seen that each flow channel is associated with the equivalent of one-half of one tube. Knowledge of channel flow conditions allows the determination of the mass flow rate of each channel. Dividing the total mass flow rate by the mass flow rate associated with each channel results in the number of flow channels needed to accommodate the total shell side mass flow rate. Dividing the number of flow channels by two results in the number of tubes required to produce the necessary number of flow channels. The mass flow rate of the brine and tube number help to define tube side flow conditions which are necessary for the heat transfer analysis.

The tube side heat transfer coefficients have been shown to increase in all sections as turbine inlet temperature increases. As turbine inlet temperature increases, the mass flow rate of the isobutane necessary to produce the desired power decreases and the number of flow channels needed to accomodate the isobutane also decreases. The number of flow channels dictates the number of tubes through which the brine flows. If the decrease in mass flow rate of the

brine was proportional to the decrease in isobutane mass flow rate, then tube side heat transfer coefficients would not vary significantly as turbine inlet temperature increased. However, the reduction in brine mass flow rate is not proportional to that of the isobutane. Figure 11 shows that the ratio of brine mass flow rate to isobutane mass flow rate increases with increasing turbine inlet temperature. Since the ratio of the brine mass flow rate to isobutane mass flow rate increases, as the turbine inlet temperature increases, there must be corresponding increases in brine velocity. The higher brine velocities result in higher tube side heat transfer coefficients.

As a consequence of variations in tube lengths and fluid velocities as the turbine inlet temperature is increased, the pressure drop experienced through the heat exchanger also varies. Figure 12 shows the relation between shell side pressure drop and turbine inlet temperature. It is seen that a minimum pressure drop occurs at a turbine inlet temperature of approximately 275°F. Note in Figure 7 that the minimum tube length occurs between turbine inlet temperatures of 290°F and 300°F. The reason for the different points of minimum can be seen by examining the curves which show the sectional variation in tube length and pressure drop as turbine inlet temperature is increased. The existence of minimums in the total tube length and total pressure drop curves can be primarily attributed to the behavior observed in the superheat and non-boiling sections.

In Figure 7 it is seen that the tube lengths associated with the different sections are of similar magnitude and until a turbine inlet temperature of approximately 295°F has been reached, the slope of the curve associated with the non-boiling section is the largest of the three curves and therefore, the behavior of the total tube length curve is dominated by the behavior of the non-boiling section. After 295°F, the slope of the curve associated with the superheat section is the largest of the three and therefore, its behavior dominates the total tube length curve. Use of similar reasoning on the pressure drop curves will show that the superheat behavior becomes dominant at approximately 275°F.

Since the minimum pressure drop occurs at 275°F and the minimum tube length occurs at 295°F, a turbine inlet temperature of 280°F was used for all other parameter studies. This temperature compromises between minimum length and minimum pressure drop.

In an effort to determine the relationship between turbine inlet temperature and the amount of tube material necessary for the construction of the heat exchanger,

products were taken of the tube lengths and the corresponding number of tubes. The resulting products are proportional to the quantity of material required, and when plotted against turbine inlet temperature, the relationship between material quantity and temperature results. The resulting tube material versus turbine inlet temperature curve is shown in Figure 7.

Material quantity is seen to decrease continuously from a maximum at the lowest turbine inlet temperature. Up to a turbine inlet temperature of 295°F, the reduction in the necessary tube material results from the decrease in tube lengths and tube number. In Figure 11, the curve relating tube number and turbine inlet temperature shows that the number of tubes required decreases throughout the turbine inlet temperature range. From Figure 11 it can be seen that the reduction in tube number is attributable to the decrease in isobutane mass flow rate as turbine inlet temperature is increased. When turbine inlet temperature becomes greater than 295°F, tube lengths are seen to increase. The increase in tube length, however, is not of a sufficient magnitude to offset the effect of tube number, which is still decreasing. Consequently, the tube material curve continues to decrease for turbine inlet temperature greater than 295°F.

Effect of Tube Diameter

Any parameter which can significantly alter flow conditions on either side of the tube will have profound effects on the design of the heat exchanger. The inside tube diameter is such a parameter and Figures 13 and 14 show the effect of the inside tube diameter on total tube length, tube number, tube material, and shell side pressure drop.

From the total tube length curve it is seen that the trend is one of increasing tube length as diameter increases. The tube length behavior is the result of the combination of two effects; the decrease in thermal resistance and the change in heat transfer requirements per tube as diameter increases.

Figure 15 shows the effect of diameter on heat transfer coefficients and for both brine and isobutane, there is a decline in heat transfer coefficients as diameter increases. The decrease in isobutane heat transfer can be attributed to the increase in channel size as diameter increases. Increases in channel size are experienced because tube pitch, or the S/D_o ratio, is kept constant and as tube diameter increases, the distance between centerlines of adjacent

tubes, S, and the equivalent flow channel diameter correspondingly increase. Single-phase heat transfer coefficients are functions of Reynolds and Prandtl numbers. Expressions for single-phase heat transfer coefficient generally have the following form:

$$H = E\ Re^{A}\ Pr^{B}\ \frac{k}{De} \tag{18}$$

where E is a proportionality constant. Since the transport properties are unaffected by tube diameter, G and Pr are fixed for all tube diameters. The equivalent diameter of the flow channel, De, increases with increasing tube diameter. Re, as can be seen from Equation (16), is proportional to De, but since the exponent A is less than one, increases in tube diameter result in decreases in H. As seen in Figure 15, tube side heat transfer coefficients are more affected by changes in tube diameter than are the shell side coefficients. The reductions in tube side heat transfer coefficients result from two factors: the increase in tube diameter and the decrease in brine velocity. With the increase in channel size, there is a decrease in tube number, which is directly proportional to the change in channel size. In Figure 15 we see a relationship where the ratio of the cross sectional area of the tube to that of the channel increases as tube diameter increases. Since the mass flow rate of the brine is directly proportional to the channel area and the tube area is increasing faster than that of the channel, as tube diameter increases, the bulk velocity of the brine must decrease as tube diameter increases. An inspection of Equations (16), (17), and (18) shows that H decreases when velocity decreases and diameter increases.

The expression for the thermal resistance between the brine and isobutane is given by:

$$R = \frac{1}{\pi D_i L H_B} + \frac{\ln\left(\frac{D_i}{D_i - 2Sc}\right)}{2\pi k_{Sc} L} + \frac{\ln\left(\frac{D_o}{D_i}\right)}{2\pi k_w L} + \frac{1}{\pi D_o L H_{SF}} \tag{19}$$

Inspection of Equation (19) indicates that reductions in heat transfer coefficients cause increases in thermal resistance. However, the increase in heat transfer area, due to the increase in diameter, more than compensates for

the reduced heat transfer coefficients and the net result is a decrease in thermal resistance as diameter increases. The lower thermal resistance permits the use of shorter tubes.

The channel area and its associated mass flow rate increase as diameter increases; consequently, the heat transfer requirement associated with each tube increases correspondingly. Associated with the increased heat transfer requirement is the need for a larger heat transfer area. This need can be satisfied by increasing tube lengths. For the conditions under consideration, the requirement for increased area due to higher heat transfer needs outweighs the effect of the reduced thermal resistance and the result is increases in tube length as diameter increases.

A factor which is of some significance in designing a heat exchanger is the amount of material required to produce the heat exchanger. Under conditions of constant tube diameter, the product of tube length and number is indicative of the relative amounts of tube material required. In this case, however, the product must also include the sum of the diameter and the tube wall thickness if an accurate indication of relative material use is to be obtained.

The tube material curve of Figure 13 shows a steady increase as tube diameter increases. The effect of the increasing tube diameter and tube length outweighs the effect of the declining tube number. Therefore, the required material quantity increases as tube diameter increases.

In Figure 14, increasing the diameter is seen to result in nearly proportional increases in total shell side pressure drop. This relationship can be attributed to the gravitational pressure drop behavior. As tube diameter is increased, the channel area and its corresponding equivalent diameter also increase. Increases in the equivalent diameter of the channel result in proportional increases in the Reynolds number. From the Moody diagram, it can be seen that the increase in Reynolds number results in slight reductions in the friction factor. Pressure drop is determined from the following equation:

$$P_{in} - P_{out} = f \gamma \frac{L}{De} \frac{V^2}{2g_c} \qquad (20)$$

Since velocity, V, is unaffected by diameter and the tube length, L, is nearly proportional to De, frictional pressure drop is proportional to the friction

factor, f. As seen in Figure 14, the decrease in frictional pressure drop is insignificant when compared to the increase in gravitational pressure drop. Gravitational pressure drops are directly proportional to tube length. Consequently, total shell side pressure drop should be nearly proportional to tube diameter.

Effect of Isobutane Velocity

Heat exchanger-related computations were performed for isobutane velocities of 4, 7, 10, and 15 feet per second. The velocity referred to in this discussion is the isobutane velocity associated with the mean temperature of the non-boiling section. The effect of velocity on tube length, pressure drop, and heat exchanger material is illustrated in Figure 16.

The total tube length is seen to increase with increasing velocity. The mass flow rate associated with each flow channel can be determined from the following equation:

$$\dot{m} = \rho AV \tag{21}$$

where A is the channel flow area. Since velocity, V, is the only variable changing, mass flow rate is proportional to V. As velocity increases, the mass flow rate of each channel increases proportionately and since the total isobutane mass flow rate is fixed, fewer channels and tubes are necessary. The lengths of the individual tubes however, must increase as velocity increases. The use of longer tubes is necessitated by the need for more heat transfer area to accommodate the increased heat transfer requirements. Since the tube size is fixed, the only way in which the required heat transfer area can be obtained is by lengthening the tubes.

Although the heat transfer requirements are exactly proportional to the mass flow rate of the isobutane, the relationship between tube length and mass flow rate is not one of exact proportionality. Increased fluid velocities on both sides of the tube result in higher heat transfer coefficients and an inspection of Equation (19) shows that reductions in thermal resistance will result. With the reduction of thermal resistance, higher heat fluxes are experienced which has the effect of reducing the necessary heat transfer area and its associated tube length.

For the velocities under consideration, the effect of tube length reduction due to reduced thermal resistance was far less significant than the effect of tube lengthening resulting from increased heat transfer requirements. Therefore, the net effect of an increase in isobutane velocity is an increase in tube length. The rate of increase in heat transfer requirements and heat transfer coefficients can be seen in Figure 17.

The pressure drop curve of Figure 16 shows that pressure drop increases as velocity increases. From Equation (20) it can be seen that frictional pressure drop increases as a function of the square of the velocity. Gravitational pressure drops increase in accordance with the tube length increases resulting from the increases in velocity. The frictional and gravitational pressure drops combine to produce increases in the total pressure drop as velocity increases.

The tube material curve of Figure 16 shows that material quantity decreases as isobutane velocity increases. This relation results from a reduction in the number of tubes required as velocity increases. The reduction experienced is inversely proportional to velocity and is of a magnitude which is significantly larger than the tube length increase dictated by the increased heat transfer requirement. Therefore, the product of the tube length and tube number, which is indicative of the amount of tube material necessary, decreases as velocity increases.

Effect of Tube Pitch

In designing a heat exchanger, one of the parameters which must be considered is pitch, where pitch is the ratio of the center-to-center distance between two adjacent tubes to the outside diameter of a single tube. Alterations in pitch will significantly affect the flow conditions of fluids passing through the heat exchanger and as a result, quantities such as tube length and pressure drop will be greatly affected.

If tube diameter is fixed, the effect of increasing the pitch is to increase the area of the flow channel, which necessitates the use of fewer but longer tubes. The effect of pitch on tube length, tube number, tube material, and pressure drop can be seen in Figures 18, 19, and 20.

The tube length versus pitch curve of Figure 18 shows an almost linear relationship between tube length and pitch. As when considering the effect of velocity variation, there are two effects which must be considered. First, there are

thermal resistance variations resulting from altered flow conditions, and second, consideration must be given to variations in length due to altered heat transfer requirements for the individual channels.

From Figure 2, it is seen that each flow channel is associated with three tubes in a triangular array. The area of this flow channel is given by:

$$A_{channel} = D_o^2 \left[pitch^2 \, (0.433) - \frac{\pi}{8} \right] \tag{22}$$

From Equation (22) it can be seen that increases in pitch result in larger flow channels. It should be noted that although the size of the flow channel changes, isobutane velocity is held constant. The larger flow channels, however, allow the mass flow rate of each channel to increase as pitch increases. Consequently, the number of flow channels decreases since the total isobutane mass flow rate is unaffected by pitch. Since tube number is proportional to the number of flow channels, tube number decreases with increasing pitch. Brine mass flow rate is fixed, so as tube number decreases, brine velocity must increase proportionately.

Since brine velocity increases as pitch increases and all other tube side heat transfer-related quantities are constant, Equations (16), (17), and (18) indicate that tube side heat transfer coefficients must increase. On the isobutane side, only variations in flow channel size are experienced. As pitch increases, the size of the flow channel and its corresponding equivalent diameter also increase. An inspection of Equations (16), (17), and (18) indicates that heat transfer coefficient decreases as equivalent diameter increases. The changes in heat transfer coefficients causes alterations in the thermal resistance between the brine and isobutane. However, the changes in thermal resistance between pitches of 1.1 and 1.25 is 13%, and between pitches of 1.25 and 1.5, it is 3%.

If the changes in thermal resistance are neglected, the heat transfer area associated with each flow channel will be proportional to the mass flow rate of the isobutane. For the conditions under consideration, the mass flow rate is directly proportional to the cross sectional area of the flow channel. Therefore, the heat transfer area is directly proportional to the cross sectional area of the flow channel. Figure 18 shows a plot of the channel area versus pitch and it is seen that this curve is similar to the total tube length curve. Since the heat transfer area is directly proportional to tube length, this behavior is expected.

One of the curves in Figure 19 illustrates the relationship between material quantity and pitch. The amount of tube material necessary is largest for the smallest pitch and decreases continuously as pitch increases. This behavior can be understood by looking at the curve which shows the relation between the number of tubes and pitch. In this figure there is a continuous decrease in tube number throughout the pitch range. The total tube length is seen to increase through the pitch range but not in magnitudes which would offset the effects of the reduced tube number, and therefore, tube material continuously decreases as pitch increases.

The total pressure drop curve of Figure 20 shows the existence of a minimum occurring at a pitch of 1.22. The occurrence of a minimum results from the interaction of two pressure drop-producing mechanisms. The first mechanism involves frictional pressure drop which is inversely related to channel size, and the second mechanism is associated with the gravitational pressure drop.

The relationship between the frictional and gravitational pressure drops, and pitch can be seen in Figure 20. Since the two contributing pressure drops are of similar magnitudes, the behavior of the total pressure drop curve will be dictated by the slopes of the component pressure drop curves. In the region bordered by pitches 1.1 and 1.22, the slope of the frictional pressure drop curve is greater than that of the gravitational pressure drop curve and as a result, the total pressure drop curve follows the trend dictated by the frictional pressure drop curve. For pitches greater than 1.22, the slope of the gravitational pressure drop curve dominates and the total pressure drop curve follows the trend it dictates. When pitch is less than 1.22, the dominant curve has a negative slope and for pitches greater than 1.22, a positive-sloped curve dominates. The result is a curve whose minimum is at a pitch of 1.22.

Effect of Scale

Largely due to its low thermal conductivity, scales must be considered as a very important factor in the design of a heat exchanger. To determine the effect of scaling on heat exchanger design, computations were performed for various scale thicknesses. Since it is not known what types of scale will form, thermal conductivities of the more common scales were examined and a mean conductivity of 0.9 Btu/hr-ft-F was obtained and used in the computations.

The curves in Figures 21 and 22 show the effect of scaling on tube length, pressure drop, and thermal resistance. The most significant effect associated

with scale growth involves the increase in thermal resistance. Because scales have such low thermal conductivities, only thin layers are necessary to significantly increase the thermal resistance between the fluids. In Figure 22 it can be seen that after a build up of only .05 in., the scale resistance comprises 95% of the total thermal resistance. Thus, for scale thicknesses greater than .05 in., the thermal resistance associated with convection becomes almost negligible. In addition, tube side heat transfer coefficients increase with the development of scales, which futher reduces the convective thermal resistance. The increase in tube side heat transfer coefficient results partly from the decrease in the inside tube diameter and partly from the increase in brine velocity, which is a consequence of the reduced diameter. From Equations (16), (17), and (18), it can be seen that the decrease in tube diameter and the increase in velocity results in higher heat transfer coefficients.

There are two opposing influences acting on the thermal resistance between the two fluids. Tube side heat transfer coefficients are increasing as scale continues to develop. The effect of this is to decrease the thermal resistance. The effect of the increasing heat transfer coefficient is offset by increasing conductive resistance. For scale thicknesses greater than .05 in., the effect of convection is negligible and thermal resistance becomes proportional to scale thickness. For scale thicknesses less than .05 in., the combination of the conductive and convective effects results in a nearly linear relationship between thermal resistance and scale thickness. Thus, thermal resistance increases almost linearly with scale thickness. Since the only variable affecting the heat exchanger is thermal resistance, total tube length will be proportional to thermal resistance, which is nearly proportional to scale thickness.

The shell side pressure drop curve of Figure 21 shows an almost linear relationship with scale thickness. This behavior is a consequence of the tube length and scale thickness relationship. Since the flow conditions on the isobutane side are unaltered by the presence of scales, frictional and gravitational pressure drops become nearly proportional to tube length. A near linear relationship exists between tube length and scale thickness. Thus, a near linear relationship between pressure drop and scale thickness must result.

Effect of Pinch Point Temperature Difference

The results described in the previous discussions were obtained by using a pinch point temperature difference of twenty degrees. This temperature

difference is a highly influential factor in determining the necessary brine mass flow rate. Factors which affect the mass flow rate of the brine will also affect the mean temperature of the brine in the various sections. It can be seen in Figures 23 and 24 that the effect of pinch point temperature difference variation on heat exchanger design is quite significant.

When the pinch point temperature difference is increased, the energy removed per unit mass of brine decreases. As a result, the brine flow rate must be increased to furnish the required amount of heat to the isobutane. Also, the reduced energy transfer per unit mass will result in higher brine temperatures throughout the heat exchanger. The increases in brine mass flow rate and temperature can be seen in Figures 23 and 24.

In Figure 23 it can be seen that tube length decreases as the pinch point temperature difference increases. The decrease in tube length can be attributed to the increase in the log mean temperature difference between the fluids and the increased tube side heat transfer coefficients. Since tube number is not a function of the pinch point temperature difference, the brine flow rate of each tube must increase because, as can be seen in Figure 23, the total brine flow rate increases as the pinch point temperature difference increases. Higher mass flow rates result in higher brine velocities, and as shown earlier, this results in higher heat transfer coefficients. The increase in the mean temperature difference between the fluids and the increased heat transfer coefficients both have the effect of increasing the heat flux through the tubes. With the increase in heat flux, smaller heat transfer areas are needed and, therefore, shorter tube lengths are possible.

Figure 24 shows that pressure drop decreases with increasing pinch point temperature difference. Since the flow conditions on the isobutane side are unchanged except for the lengths of the various sections, pressure drop is a function of length only. An examination of the tube length and pressure drop curves shows that similar relationships exist between the aforementioned quantities and pinch point temperature difference.

Tube number is not a function of the pinch point temperature difference. As a result, tube material is exactly proportional to tube length.

It has been shown that tube length, tube material, and pressure drop decrease as the pinch point temperature difference increases. Reduction in these quantities is desirable since lower heat exchanger costs usually result.

This cost relationship compels the use of high pinch point temperature differences. Therefore, a pinch point temperature difference of twenty degrees was used in all other parameter studies. Higher temperature differences may result in excessive brine flow rates and tube side pressure drops.

Effect of Pressure

The critical pressure of isobutane is 529 psia, so a system pressure of 600 psia was used in the computational procedure to determine the effect of supercritical pressure on heat exchanger design. In Figure 25, the effect of pressure on cycle efficiency can be seen as the turbine inlet temperature is varied. The differences between the subcritical and supercritical efficiency curves will produce significant behavior differences in the respective tube length, tube material, and pressure drop curves. The aforementioned curves are shown in Figures 26, 27, and 28.

Figure 26 shows that tube length continuously increases as the turbine inlet temperature increases. Examination of the tube length curves associated with the subcritical and supercritical temperature sections will explain the behavior of the total tube length curve. Up to a temperature of 275°F, which is the critical temperature of isobutane, the total tube length curve follows the tube length curve of the subcritical temperature section since no supercritical section exists. For turbine inlet temperatures greater than 275°F, a supercritical temperature section does exist and its contribution causes the total length curve to diverge from the subcritical temperature curve. When turbine inlet temperature becomes greater than 290°F, the tube lengths associated with the subcritical temperature section begin to decrease, while the tube lengths of the supercritical temperature section continue to increase. This results in the formation of a plateau in the total tube length curve as turbine inlet temperature exceeds 290°F.

The decrease in tube length observed in the subcritical temperature section can be attributed to increases in the mean brine temperature of the section. The brine temperature curves in Figure 29 illustrates the increases in temperature. When turbine inlet temperature exceeds 290°F, the rate of increase of the brine exit temperature becomes significantly higher than the rate of decrease of the brine temperature at the critical point. This results in higher mean brine temperatures in the subcritical temperature section.

The increase in exit brine temperature results from the change in the brine conditions in the supercritical temperature section. As a consequence of the changed brine conditions, the ratio of the isobutane mass flow rate to brine flow rate, as can be seen in Figure 30, decreases. An examination of Figure 11 shows that as turbine inlet temperature increases, the mean temperature difference between the fluids in the supercritical temperature section decreases. Consequently, more brine is needed to supply the necessary heat to each unit mass of isobutane. The brine temperature at the location where isobutane is at its critical temperature decreases as turbine inlet temperature increases. As turbine inlet temperature increases, brine flow rate is increasing at a rate which is high enough to offset the effect of the cooler brine entering the subcritical temperature section. Therefore, the amount of energy available to each unit mass of isobutane in the subcritical temperature section increases as turbine inlet temperature increases. Once turbine inlet temperature exceeds the critical temperature, the energy requirements per unit mass of isobutane in the subcritical temperature section remain constant. Therefore, the energy level and the temperature of the brine leaving the heat exchanger increases with increasing turbine inlet.

The increases in tube length experienced in the supercritical temperature section can be attributed to increasing heat transfer requirements and decreasing mean brine temperature, as turbine inlet temperature increases. Although the total isobutane mass flow rate may be changing with turbine inlet temperature, the number of tubes is changing in a manner such that the isobutane mass flow rate associated with each tube remains constant. However, the enthalpy change across the supercritical temperature section increases as turbine inlet temperature increases. As a result, the heat transfer requirements of each tube increases as turbine inlet temperature increases. Examination of Equation (15) indicates that reductions in temperature difference results in decreases in the heat flux through the tube. There is an increase in conductance, U, resulting from increases in heat transfer coefficients, but the effect of the increased conductance is overshadowed by the decrease in temperature difference (see Figure 31 for heat transfer coefficient behavior). Therefore, heat flux through the tube diminishes as turbine inlet temperature increases. This coupled with the increased heat transfer requirements necessitates the use of longer tubes in the supercritical temperature section.

In the subcritical temperature section, both conductance and temperature difference increase with increasing turbine inlet temperature. This results in higher heat fluxes through the tube. Since the heat transfer requirement in this section is generally constant, the increase in heat flux allows the use of shorter tubes in this section.

The tube material curve of Figure 27 illustrates the variation of material quantity with turbine inlet temperature. The undulating behavior of the tube material curve results from the relationships of tube number and tube length with turbine inlet temperature. The tube number versus turbine inlet temperature curve follows trends which are essentially the inverse of those followed by the efficiency curve. This relationship is to be expected since the mass flow rate of the secondary fluid is essentially inversely related to efficiency and for the conditions under consideration, the mass flow rate of the secondary fluid dictates the number of tubes to be used in the heat exchanger. Multiplying tube number by the corresponding tube lengths yields the amount of tube material necessary.

The behavior to total pressure drop and its components is illustrated in Figure 28. The gravitational and subcritical frictional pressure drop curves both show decreases in pressure drop after reaching a maximum. In both cases, the decrease can be attributed to the decrease in tube length experienced in the subcritical temperature section as turbine inlet temperature becomes greater than 290°F. Shell side flow conditions are fixed in the subcritical temperature section for turbine inlet temperatures greater than the critical temperature of the secondary fluid. The frictional pressure drop of this section becomes a function of the tube length alone and follows the trends dictated by the tube length curve of the subcritical temperature section. The total gravitational pressure drop results from a sum of the gravitational components associated with the subcritical and supercritical temperature sections. In Figure 26 it can be seen that after the turbine inlet temperature exceeds 305°F, the rate of decrease in tube length of the subcritical temperature section is approximately equal to the rate of increase of the tube lengths associated with the supercritical section. The mean density of the isobutane is greater in the subcritical temperature section than in the supercritical temperature section. Consequently, the decrease in gravitational pressure drop in the subcritical temperature section is greater than the increase in gravitational pressure drop associated with the

supercritical temperature section. Therefore, gravitational pressure drop decreases as turbine inlet temperature further exceeds 305°F. The increase in the frictional pressure drop of the supercritical temperature section results from the increases in tube length and mean velocity of this section. A summation of the component pressure drops results in the total pressure drop relation seen in Figure 27.

CONCLUDING REMARKS

The following conclusions were drawn from the results of the subcritical pressure and supercritical pressure cases:

1. Systems using supercritical pressures will require significantly more tube material than systems employing subcritical pressures.
2. Pumping requirements will generally be less for supercritical pressure conditions than for subcritical pressure conditions.

Under subcritical pressure conditions, variations in turbine inlet temperature will produce the following effects:

1. Tube lengths change significantly in the non-boiling and superheat sections, where they respectively decrease and increase as turbine inlet temperature increases.
2. The total shell side pressure drop will change significantly as turbine inlet temperature is varied.
3. An increase in the turbine inlet temperature will result in a decrease in the required quantity of tube material.

Conclusions concerning the effect of inside tube diameter are as follows:

1. Increasing the inside tube diameter will bring about nearly proportional increases in total tube length and total shell side pressure drop.
2. The quantity of tube material necessary will increase if tube diameter is increased.

The effect of pitch was considered and the following conclusions were drawn:

1. Total tube length will increase as pitch increases.
2. Frictional and gravitational pressure drops are similar in magnitude, but the relations between frictional pressure drop and pitch is the inverse of that associated with gravitational pressure drop and pitch.

3. The quantity of tube material required will decrease as pitch increases.

Consideration of the effect of scaling resulted in the following observations:

1. The presence of scale greatly increases the thermal resistance between the brine and isobutane.
2. Total tube length and total shell side pressure drop increase almost proportionately with scale thickness.
3. Since tube number is unaffected by the presence of scale, required tube material quantity is proportional to tube length.

Consideration of the effect of pinch point temperature difference led to the following conclusions:

1. Brine mass flow rate increases as the pinch point temperature difference increases.
2. An inverse relationship exists with pinch point temperature difference for both total tube length and total shell side pressure drop.
3. Since tube number is not a function of pinch point temperature difference, tube material quantity is proportional to tube length, and therefore has an inverse relationship with pinch point temperature difference.

REFERENCES

1. Moskvicheva, V.N. and Popov, A.E., "Geothermal Power Plant on the Paratunka River," *GEOTHERMICS*, Vol. 2, Part 2, p. 1560-1566. Proceedings of the U.N. Symposium on the Development and Utilization of Geothermal Resources, 1970.

2. Ichikawa, S., "Use of Fluorocarbon Turbine in Chemical Plants," *CHEMICAL ECONOMY AND ENGINEERING REVIEW*, October, 1970.

3. Holt, B., Hutchinson, A.J.L., and Cortez, D.H., "Advanced Binary Cycles for Geothermal Power Generation," Tenth Annual Technical Meeting, American Institute of Chemical Engineers, Southern California Section, April 24, 1973.

4. Anderson, J.H., "A Vapor Turbine Geothermal Power Plant," *GEOTHERMICS*, Vol. 2, Part 2, p. 1530-1532. Proceedings of the U.N. Symposium on the Development and Utilization of Geothermal Resources, 1970.

5. Chen, J.C., "Correlation for Boiling Heat Transfer to Saturated Fluids in Convective Flow," *INDUSTRIAL AND ENGINEERING CHEMISTRY, PROCESS, DESIGN AND DEVELOPMENT*, Vol. 5, No. 3, July 1966, p. 322-329.

6. Dengler, C.E. and Addoms, J.N., "Heat Transfer Mechanism for Vaporization of Water in Vertical Tubes," Chem. Eng. Progress, Symposium Ser. 52, No. 18, 1956, p. 95-103.

7. Guerrieri, S.A. and Talty, R.D., "Heat Transfer to Organic Liquids in Single Tube, Natural Circulation, Vertical Tube Boiler," Chem. Eng. Progress, Symposium Ser. 52, No. 18, 1956, p. 69-77.

8. Schrock, V.E. and Grossman, L.M., "Forced Convection Boiling in Tubes," *NUCLEAR SCIENCE AND ENGINEERING*, Vol. 12, 1962, p. 474-481.

9. Hawaii Geothermal Project Engineering Program, Quarterly Report No. 2, December 1, 1973, p. 26-68.

10. Kays, W.M., *CONVECTIVE HEAT TRANSFER AND MASS TRANSFER*, McGraw-Hill Book Co., Inc., 1966, p. 173.

11. Forster, H.K. and Zuber, N., "Dynamics of Vapor Bubbles and Boiling Heat Transfer," *AIChE JOURNAL*, Vol. 1, No. 4, 1955, p. 531.

12. Streeter, V.L., *FLUID MECHANICS*, Fifth Edition, McGraw-Hill Book Co., Inc., 1971, p. 292.

13. Wallis, G.B., *ONE-DIMENSIONAL TWO-PHASE FLOW*, McGraw-Hill Book Co., Inc., 1969, p. 28-29.

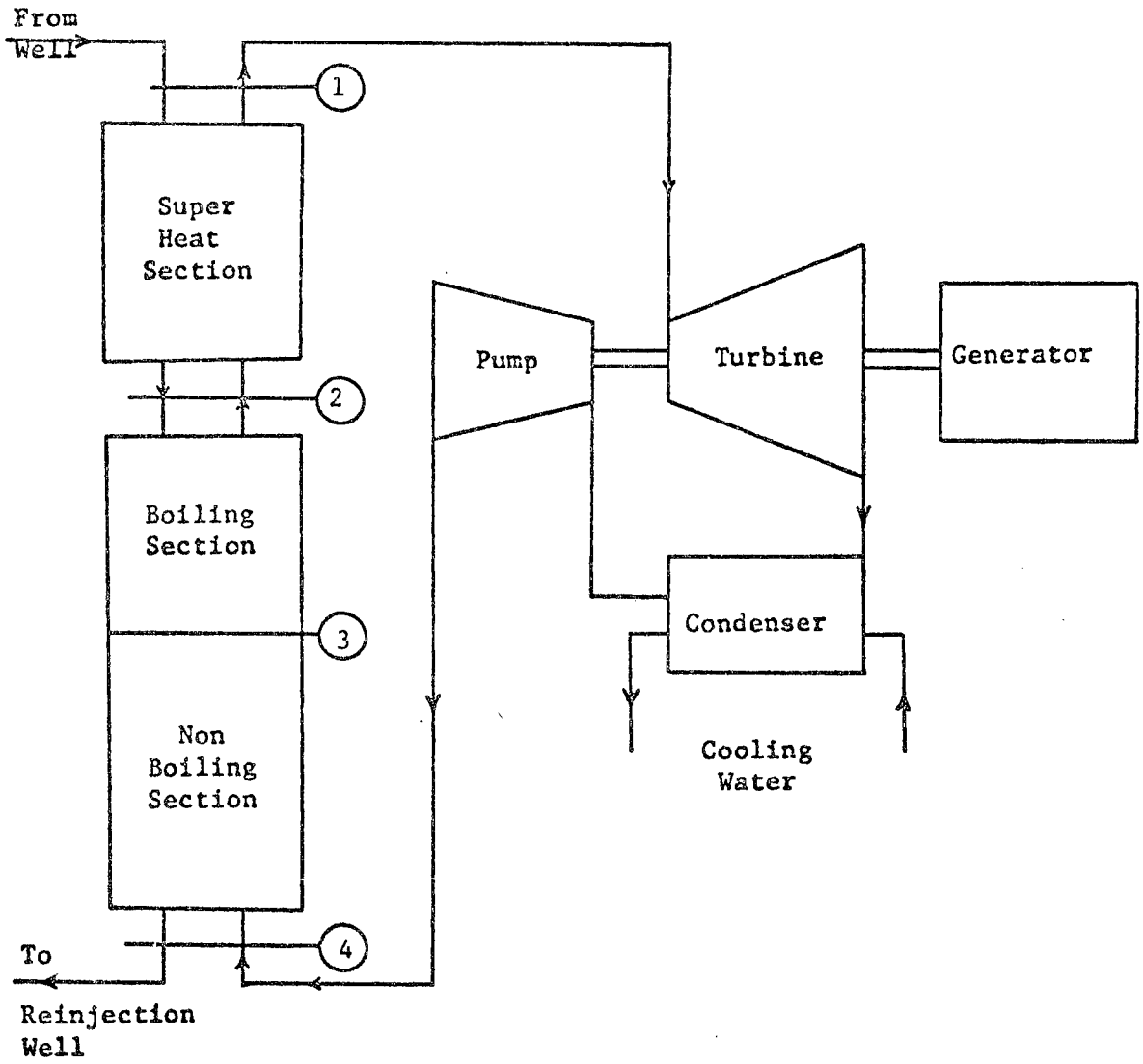

Figure 1 Schematic of Rankine Cycle with Heat Input from Hot Brine

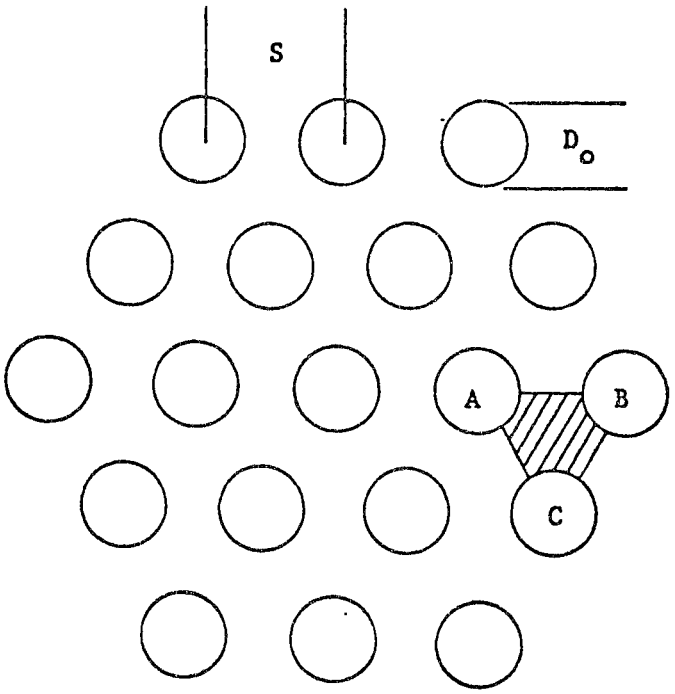

Figure 2 Tube Arrangement of the Heat Exchanger

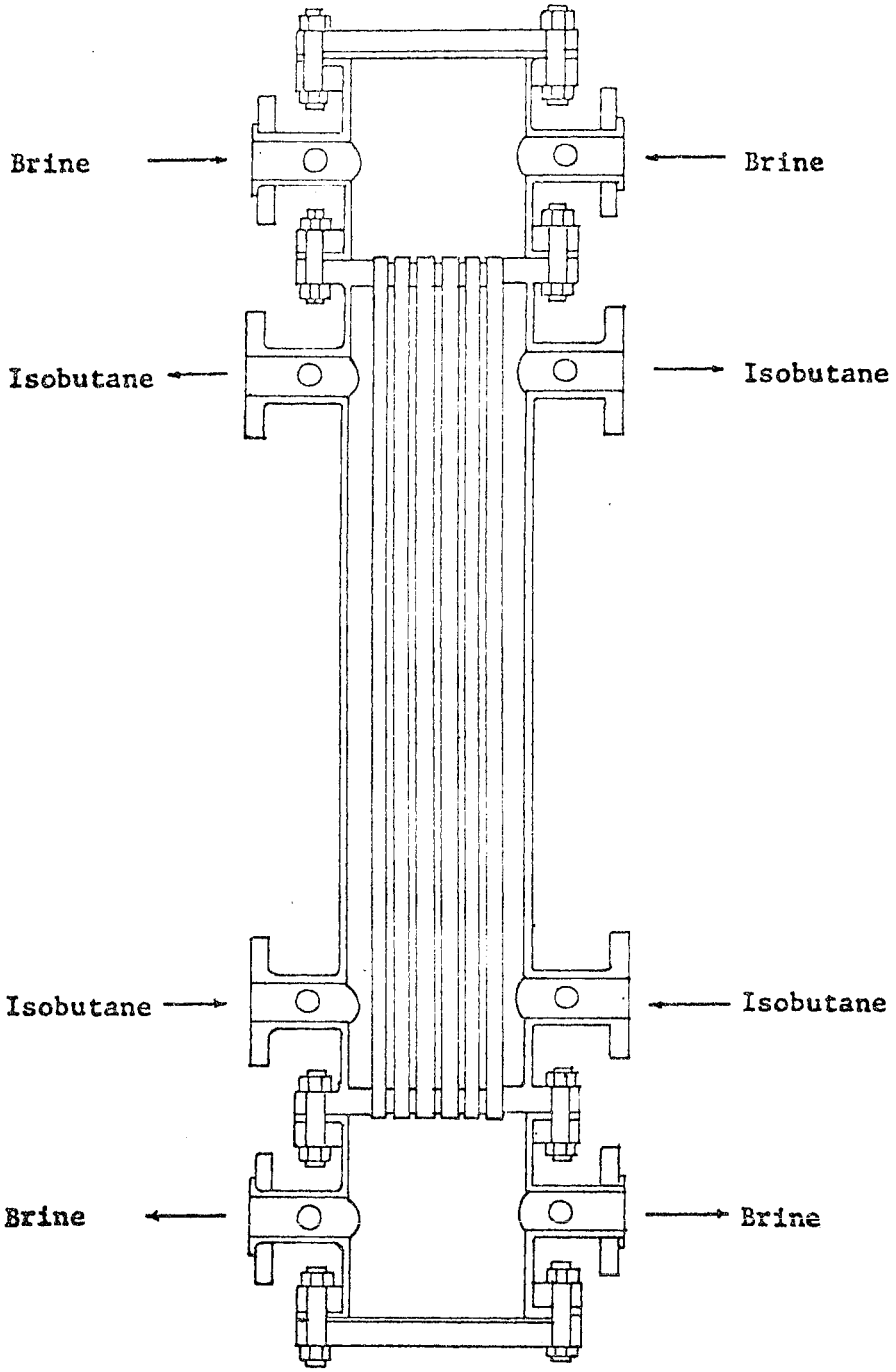

Figure 3 Cross Sectional View of the Heat Exchanger

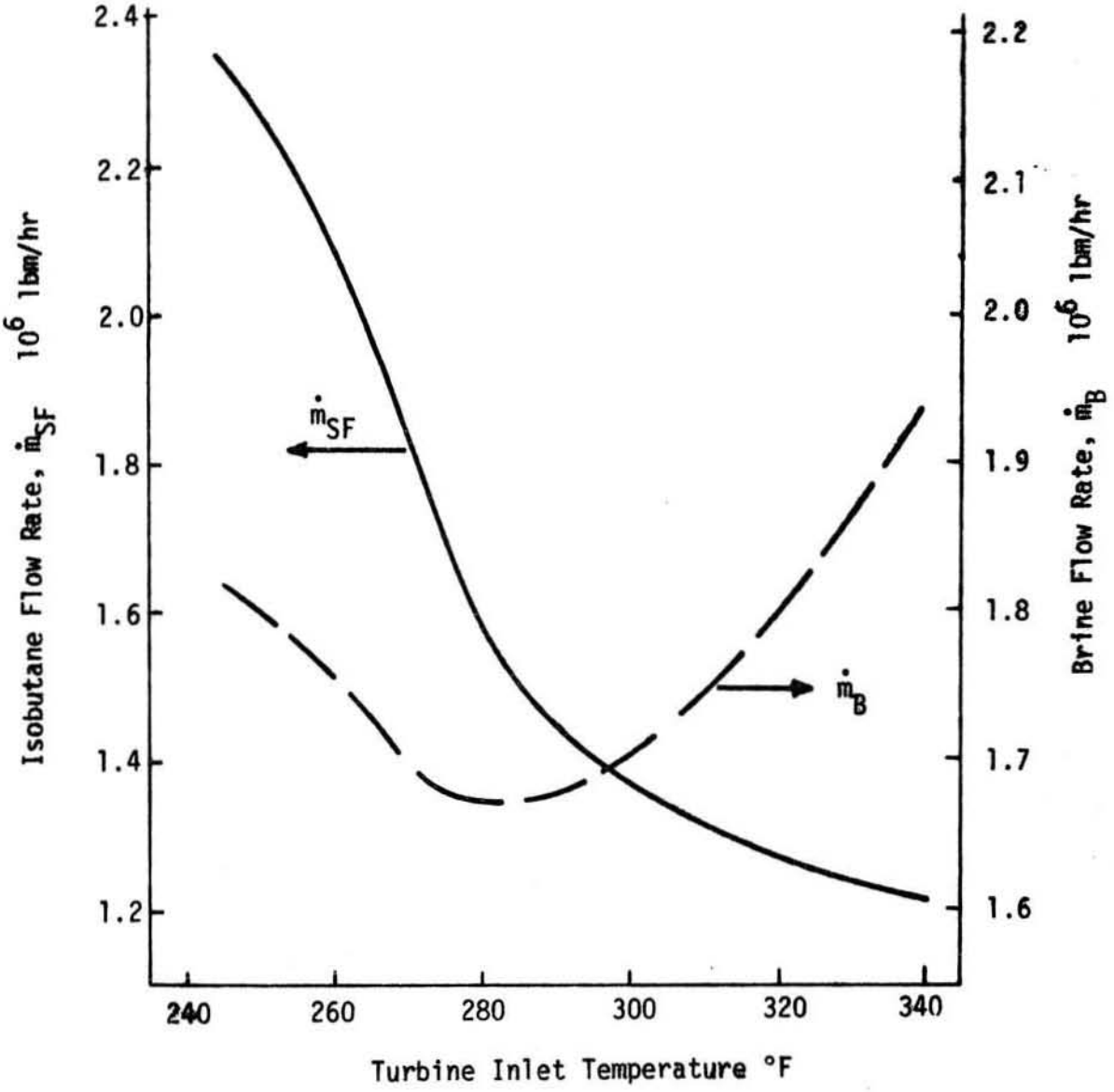

Fig. 4 Effect of Turbine Inlet Temperature on Isobutane and Brine Flow Rates

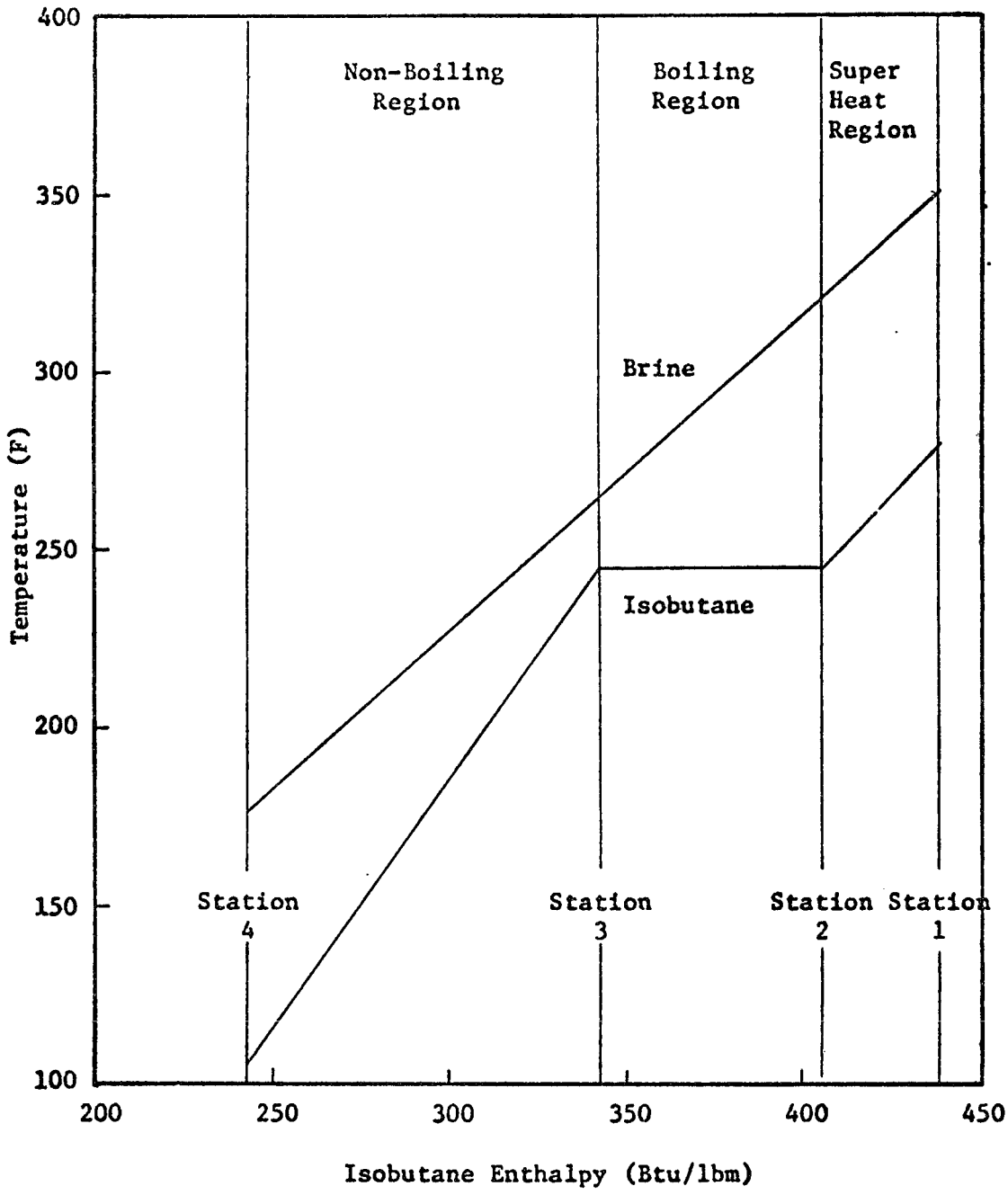

Figure 5 Temperature-Enthalpy Relationship of Brine and Isobutane for a System Pressure of 400 psia

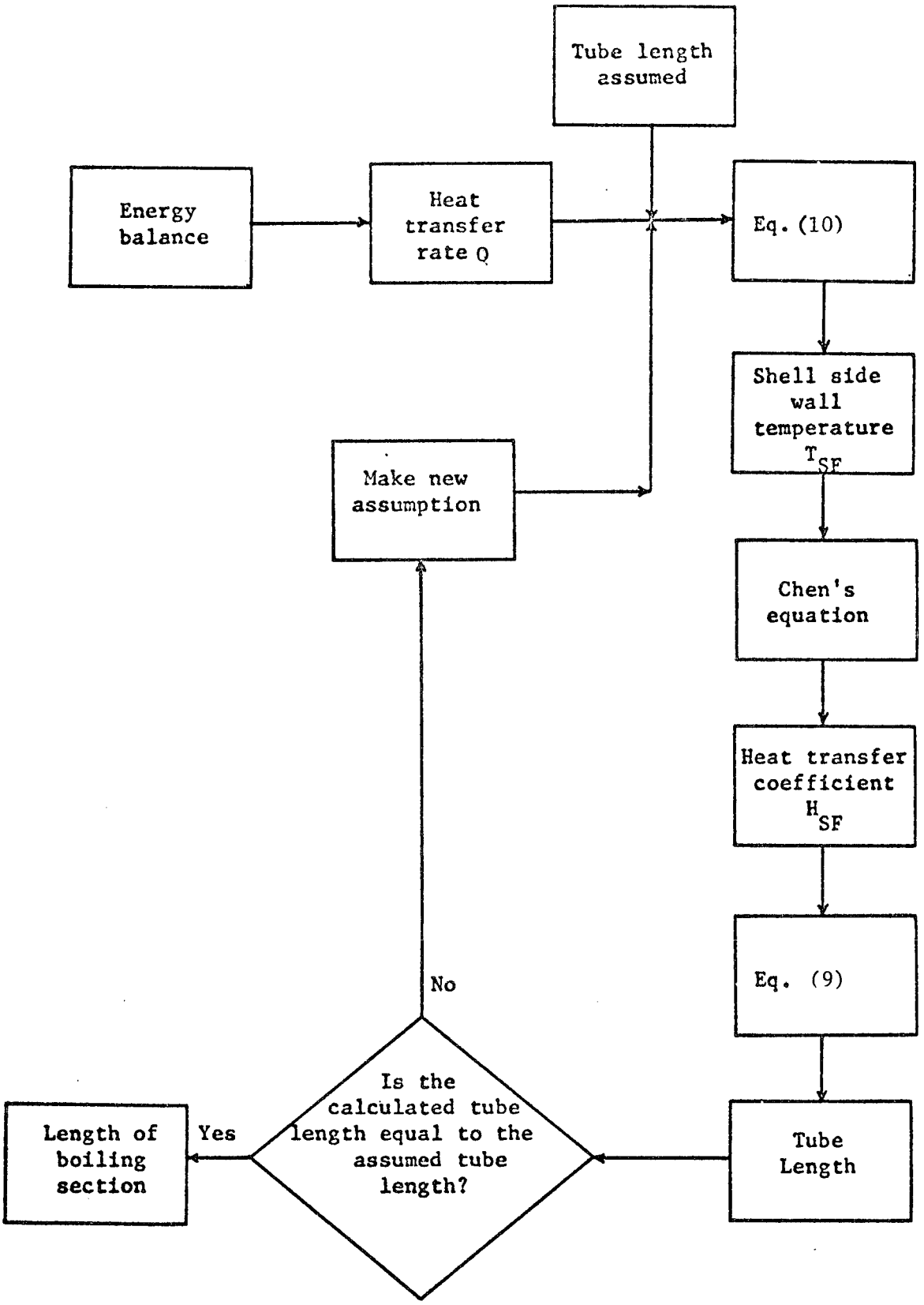

Figure 6 Flowchart of the Procedure Used to Determine Tube Lengths of the Boiling Section

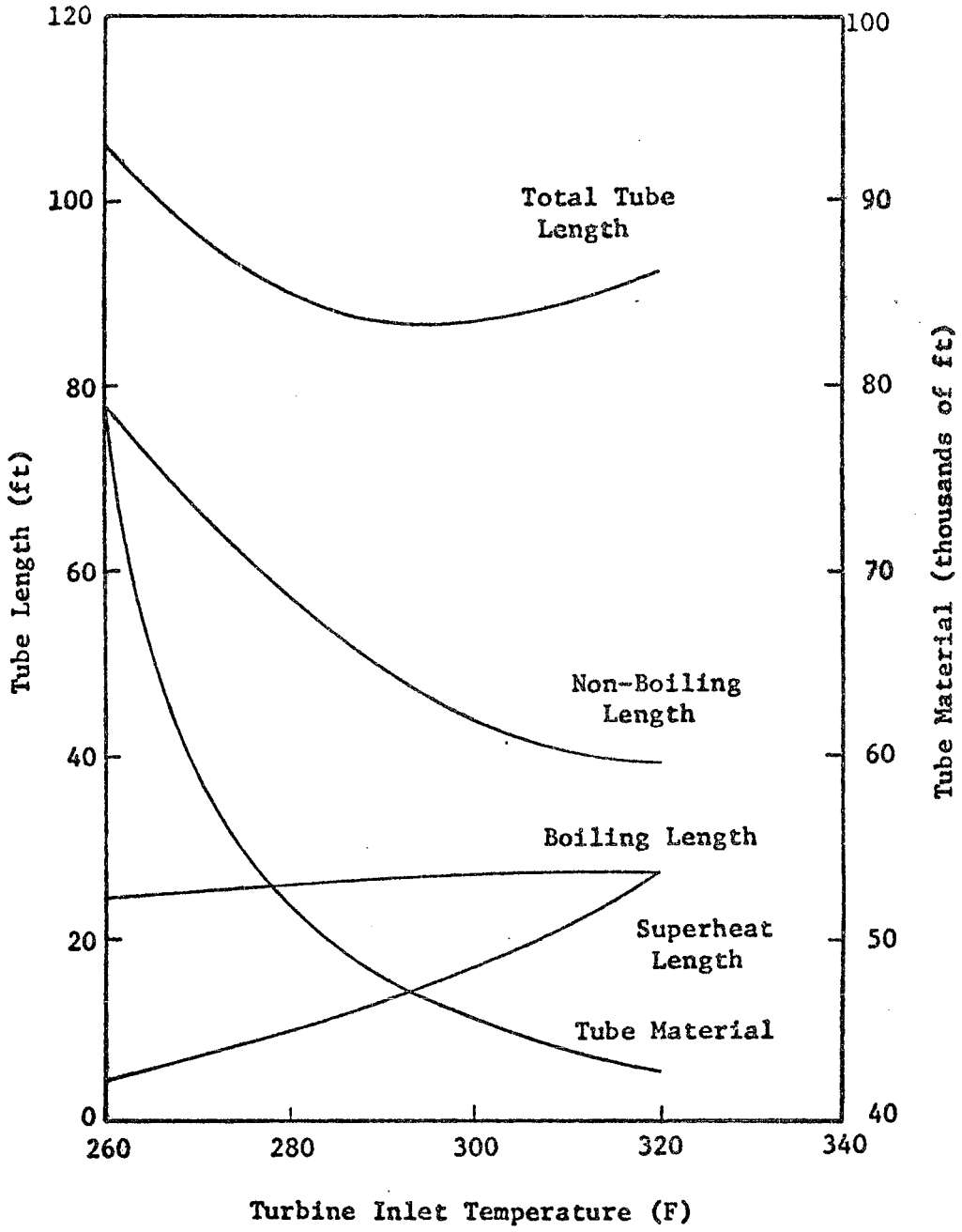

Figure 7 The Effect of Turbine Inlet Temperature on Tube Lengths and Tube Material

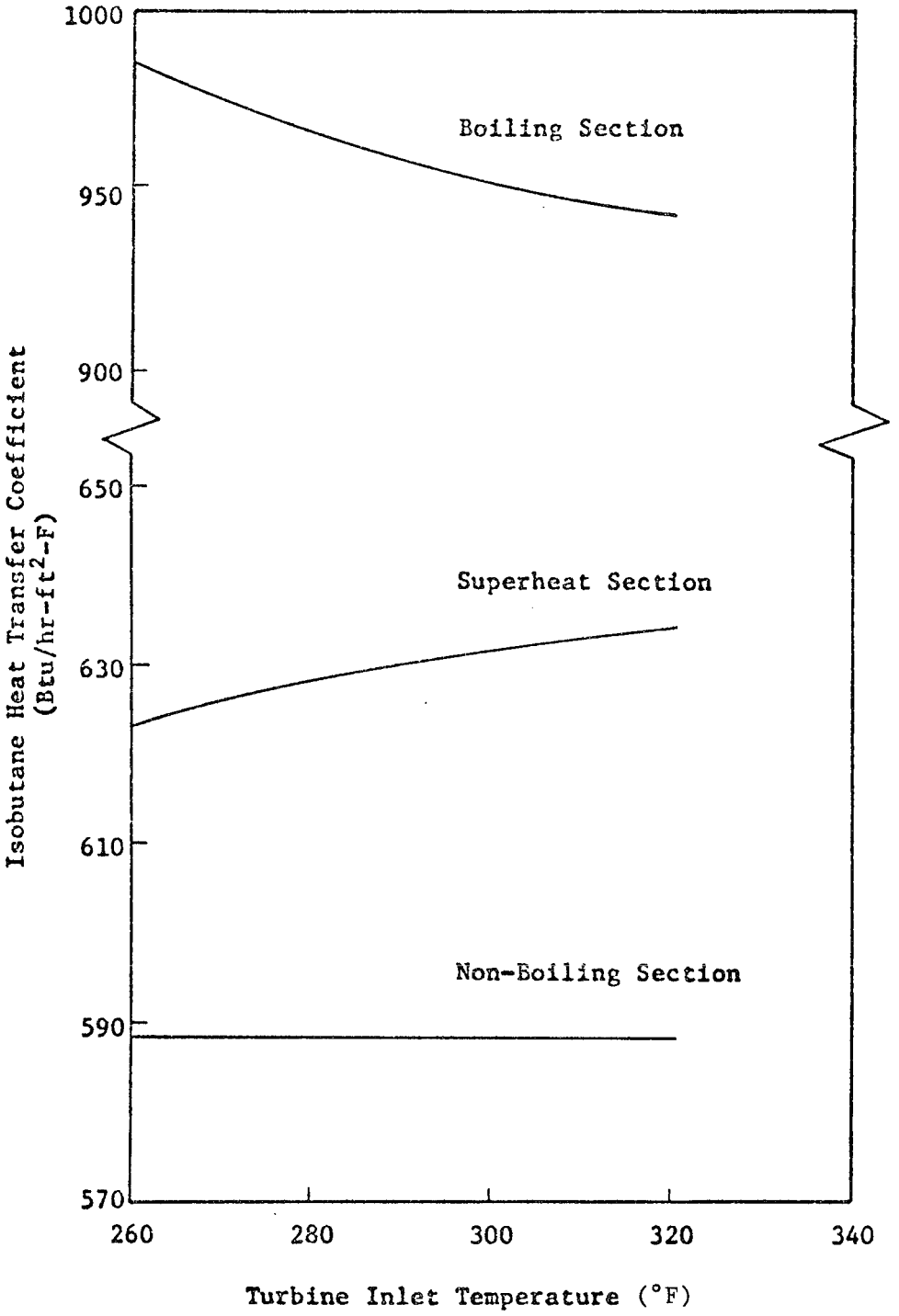

Figure 8 Shell Side Heat Transfer Coefficients
(Note: Scale change for boiling coefficient)

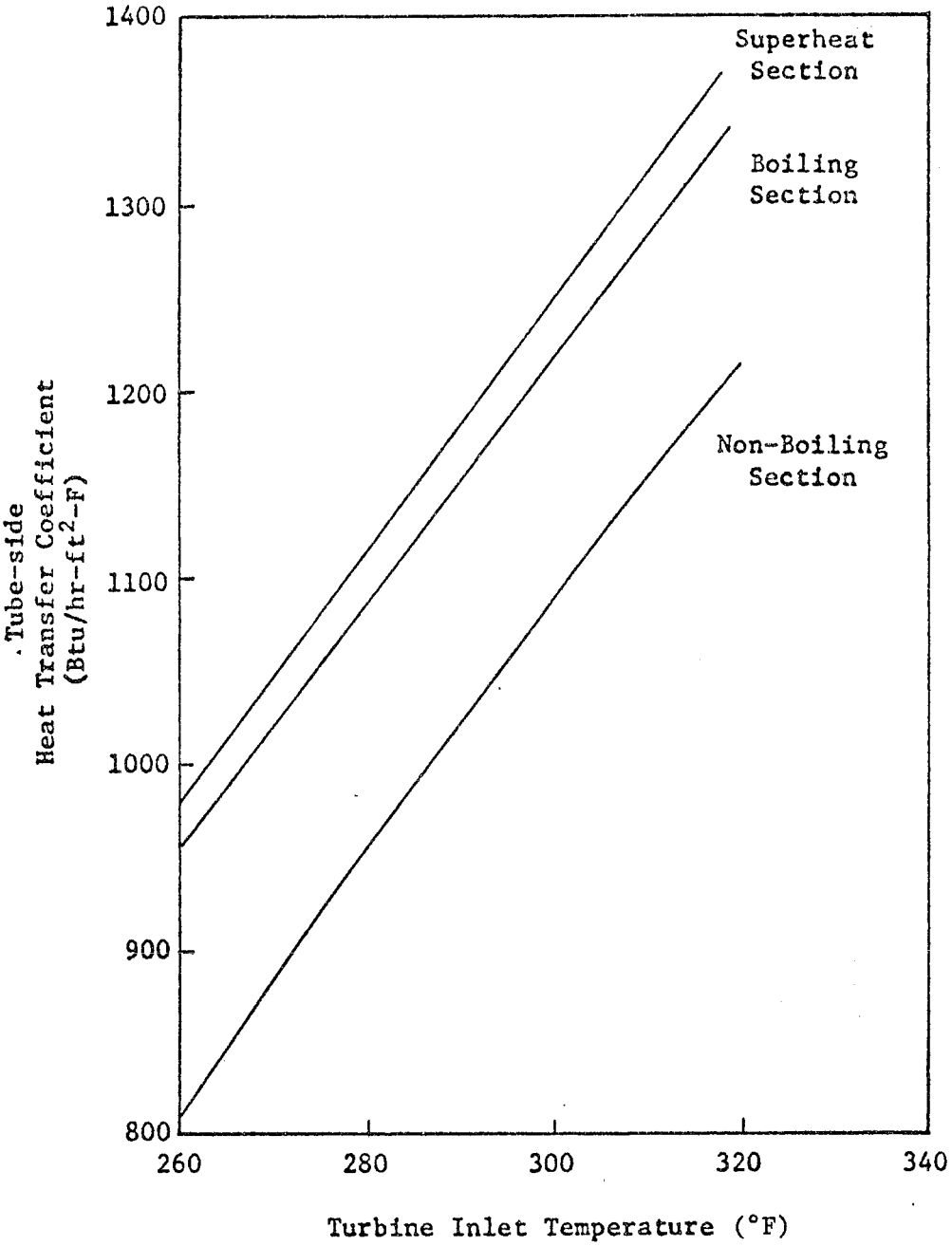

Figure 9 The Effect of Turbine Inlet Temperature on Tube-side Heat Transfer Coefficients

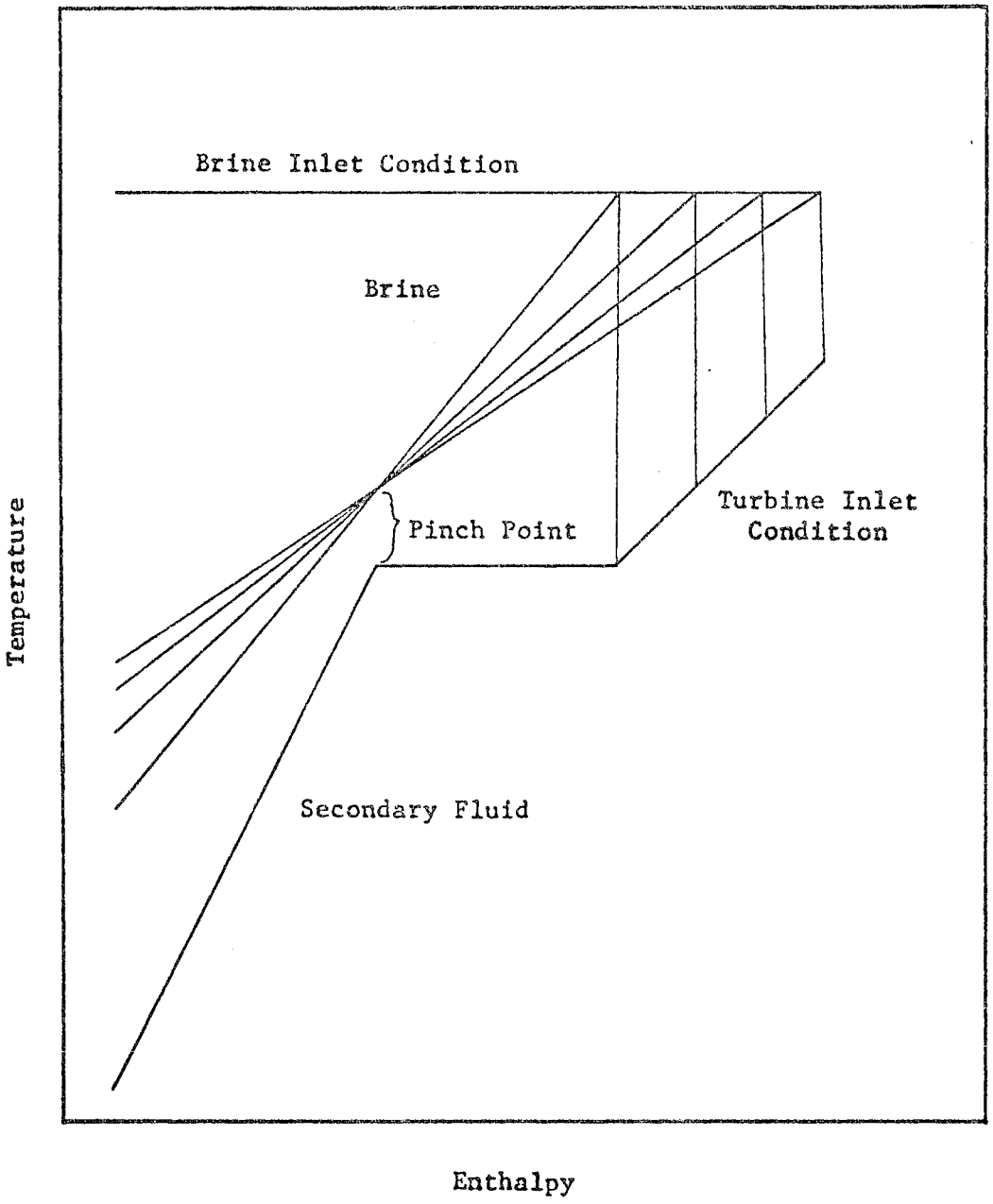

Figure 10 The Effect of Turbine Inlet Condition on Brine Conditions

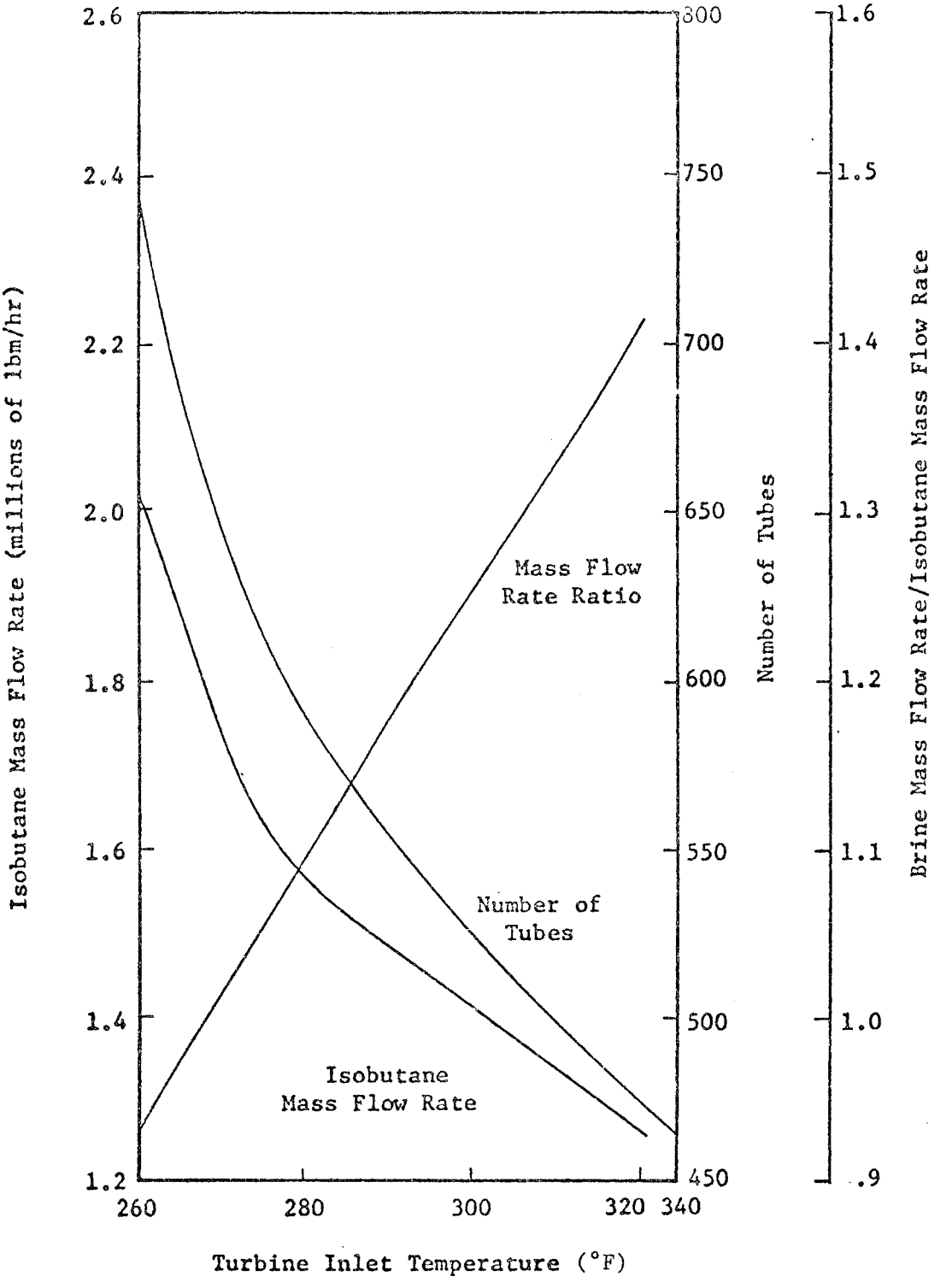

Figure 11 The Effect of Turbine Inlet Temperature on Mass Flow Rates and Tube Number

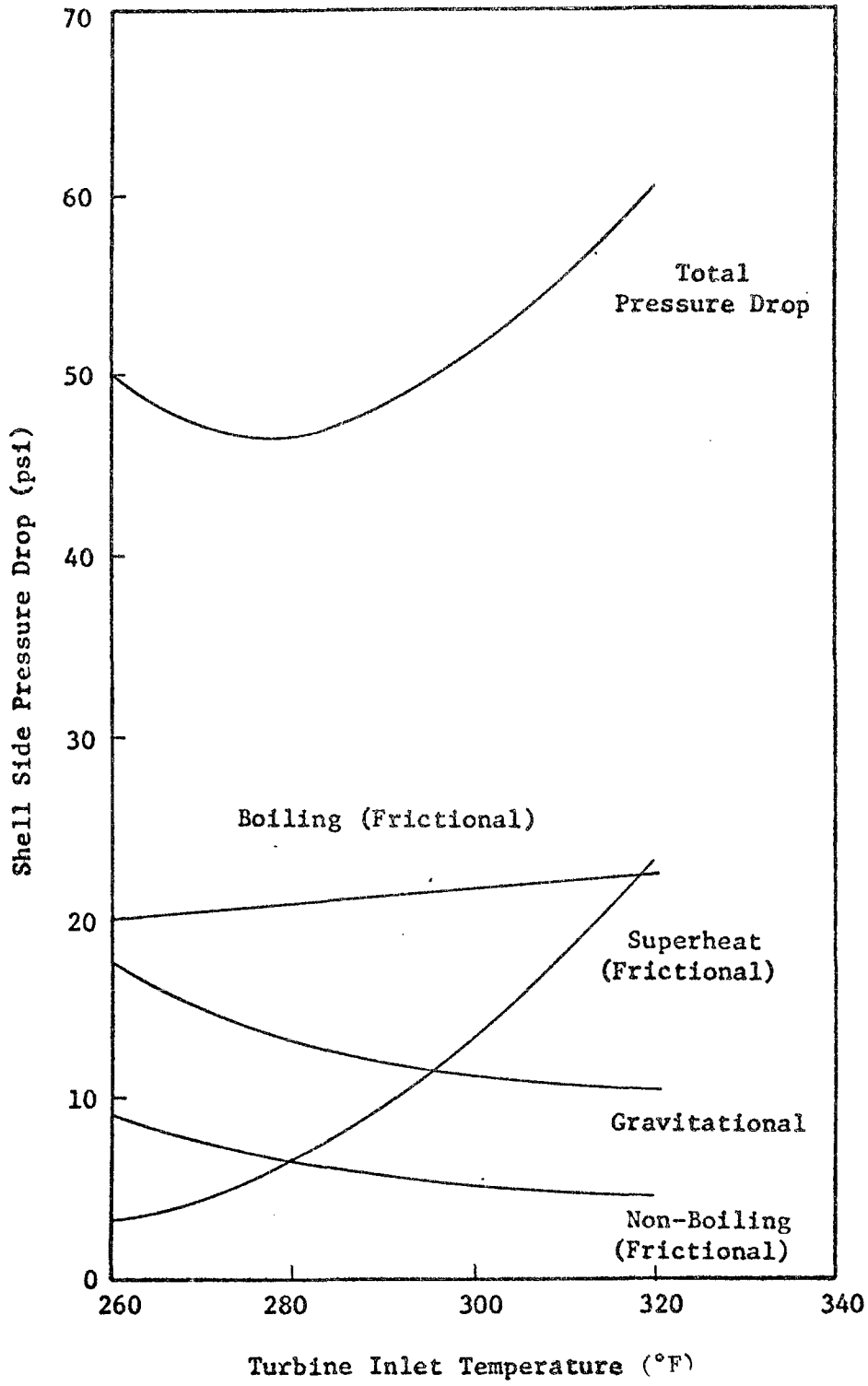

Figure 12 Shell Side Pressure Drop

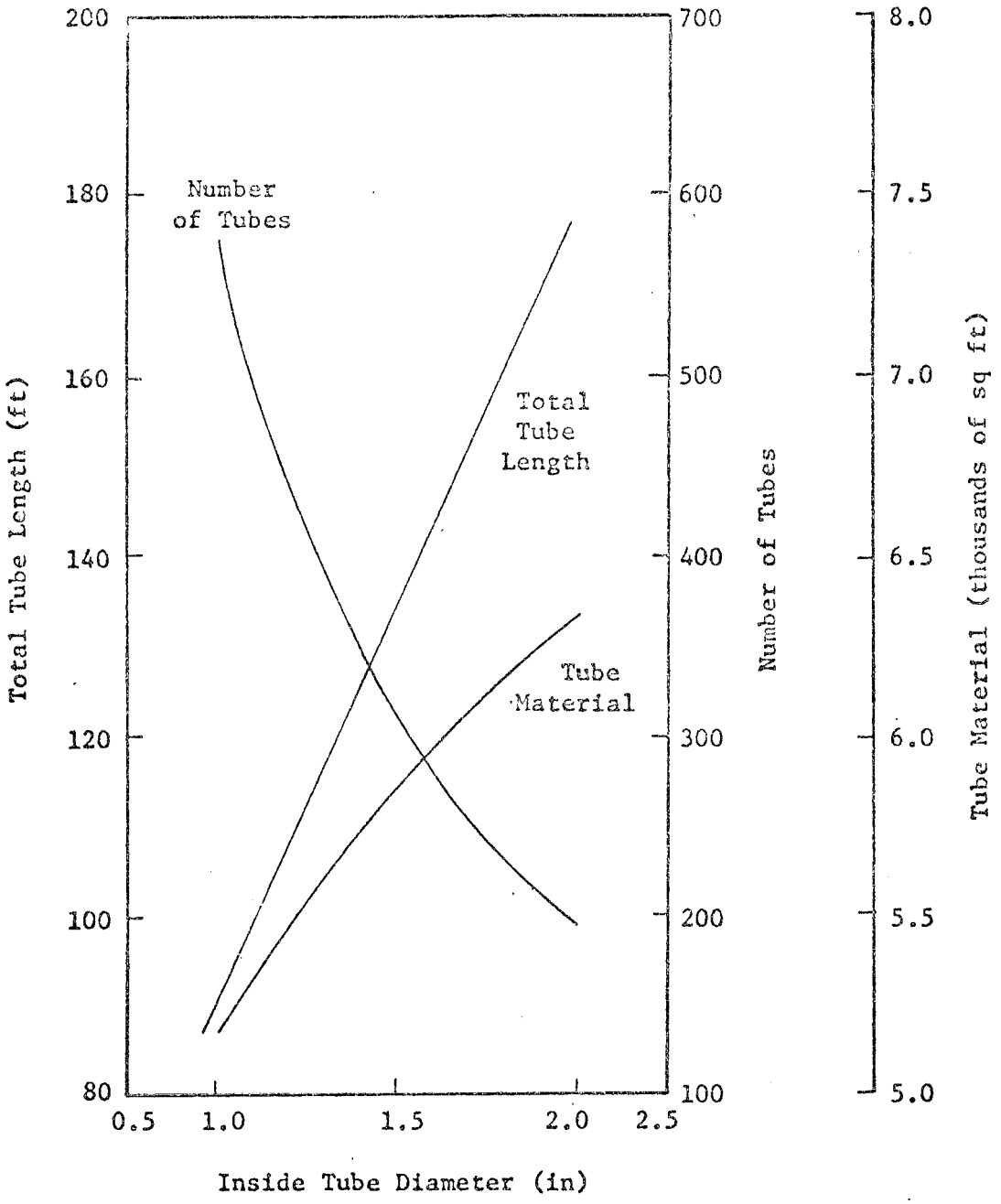

Figure 13 The Effect of Tube Diameter on Tube Length, Number of Tubes and Tube Material

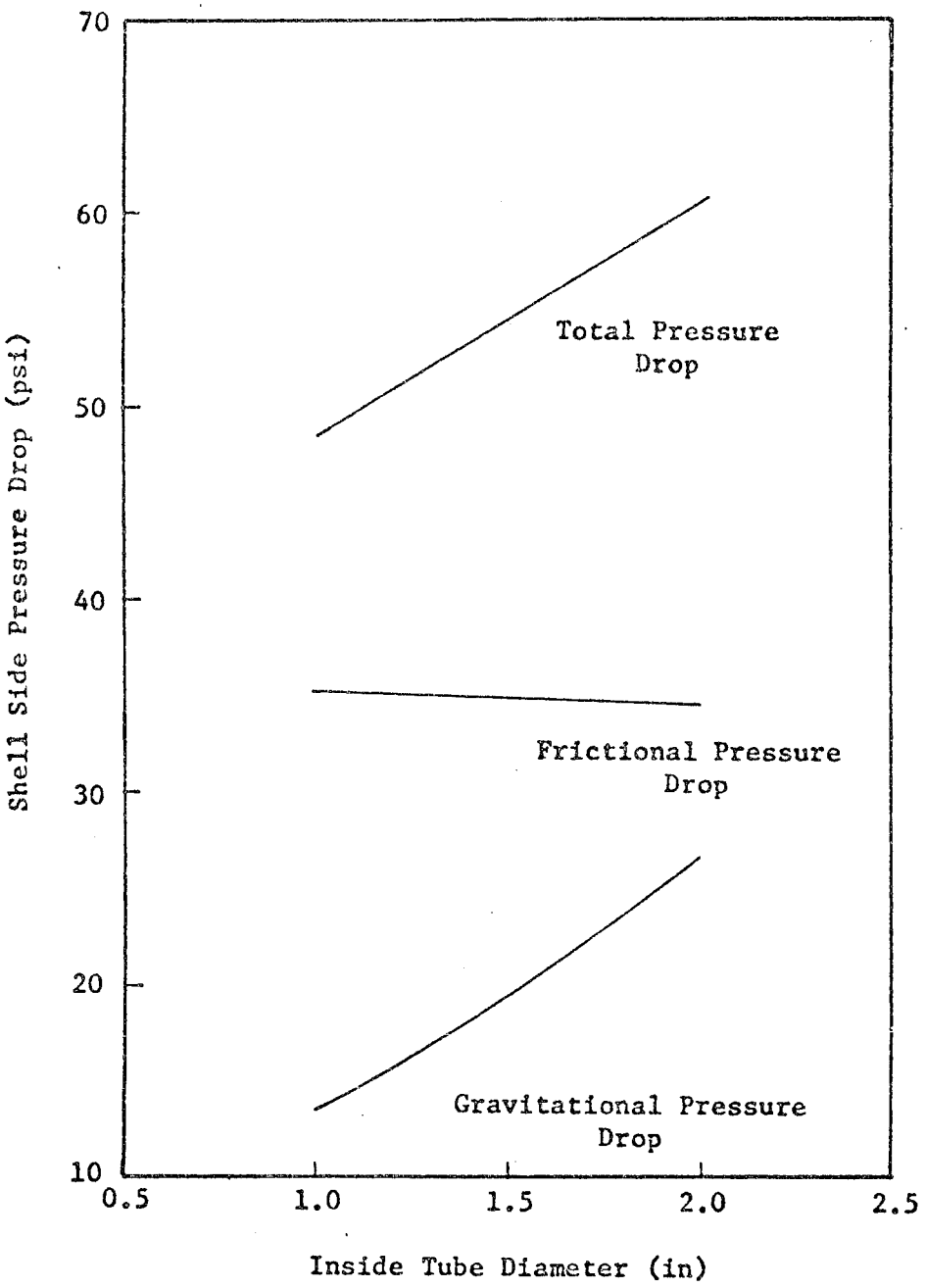

Figure 14 The Effect of Tube Diameter on Shell Side Pressure Drop

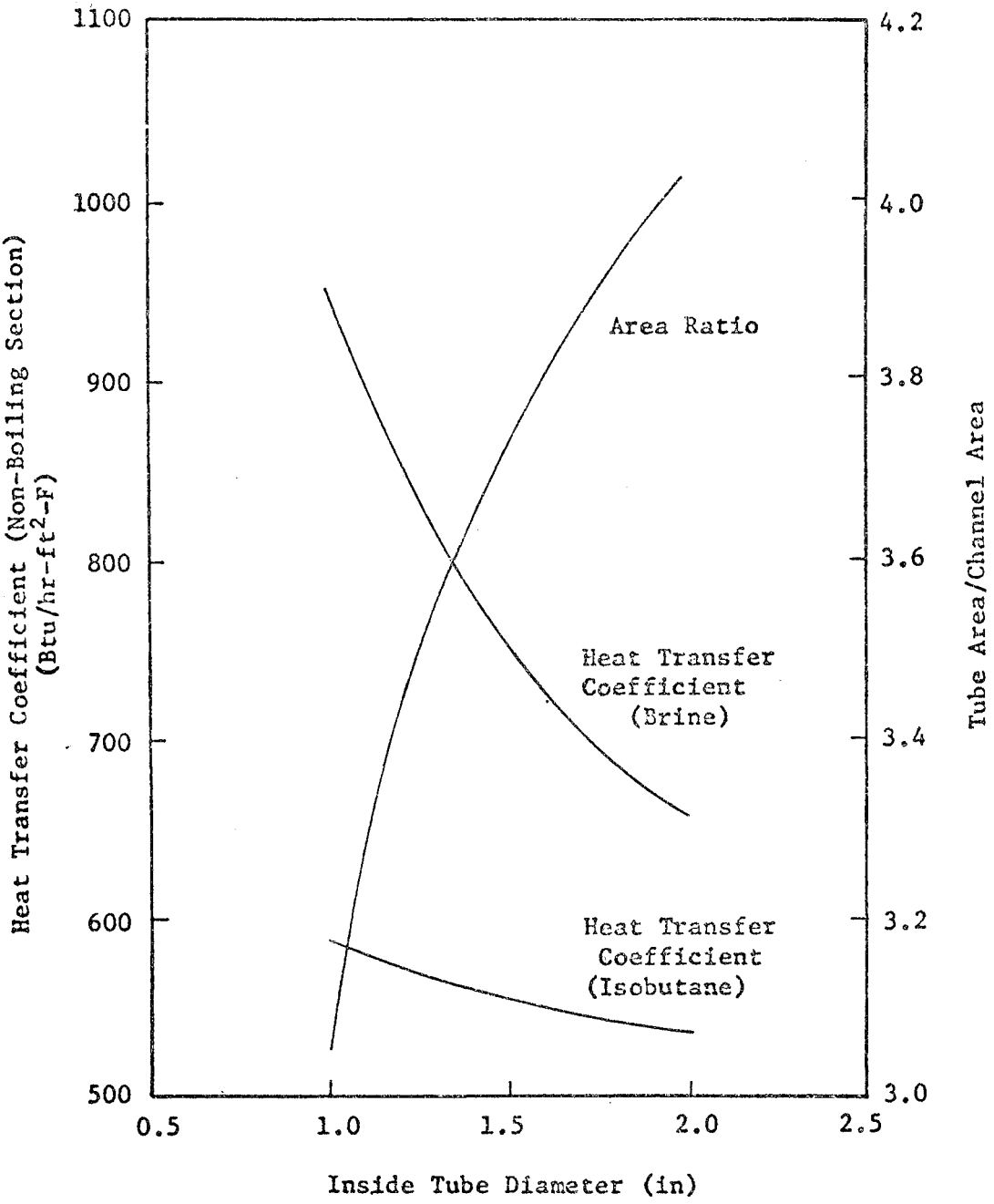

Figure 15 The Effect of Tube Diameter on Heat Transfer Coefficients and Flow Areas

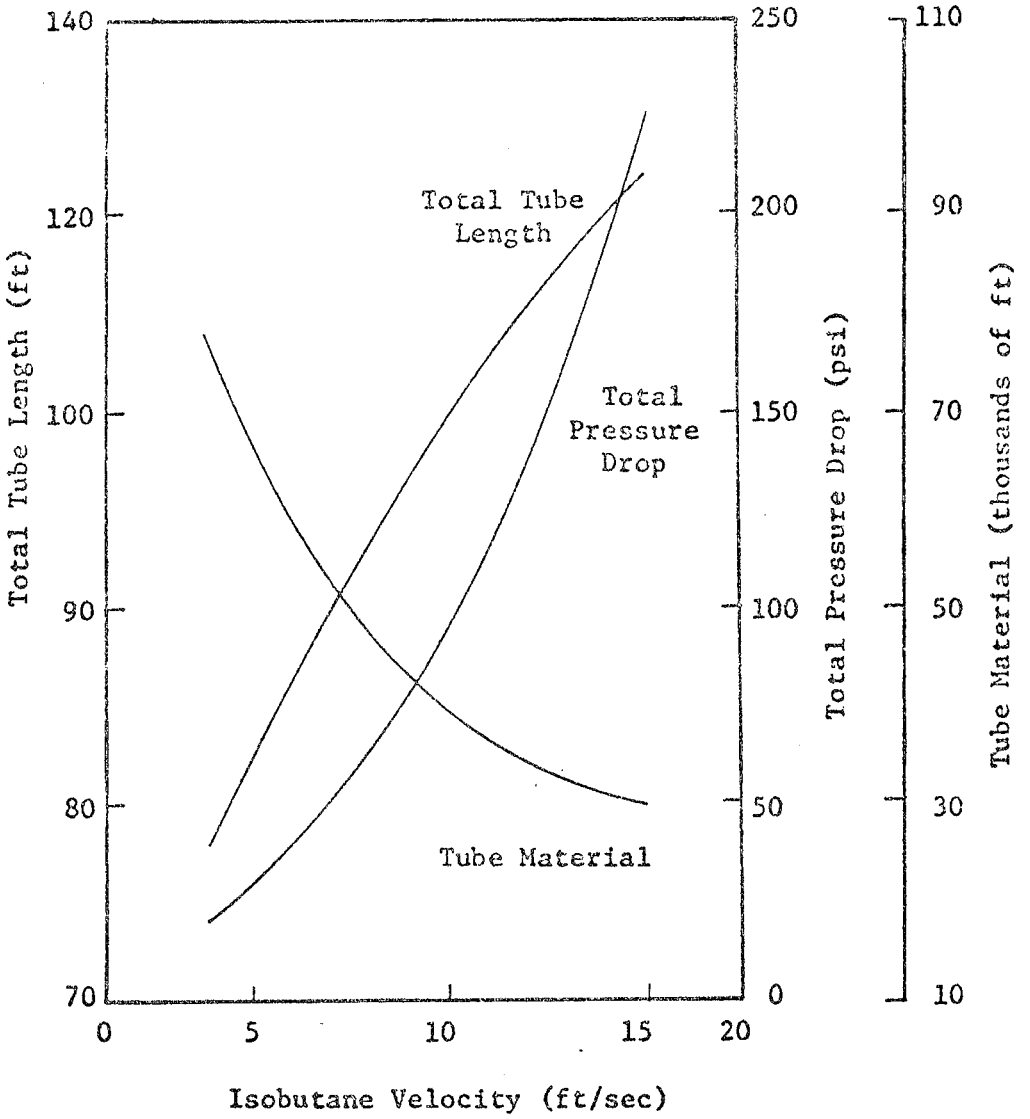

Figure 16 Effect of Isobutane Velocity on Tube Length, Pressure Drop and Tube Material

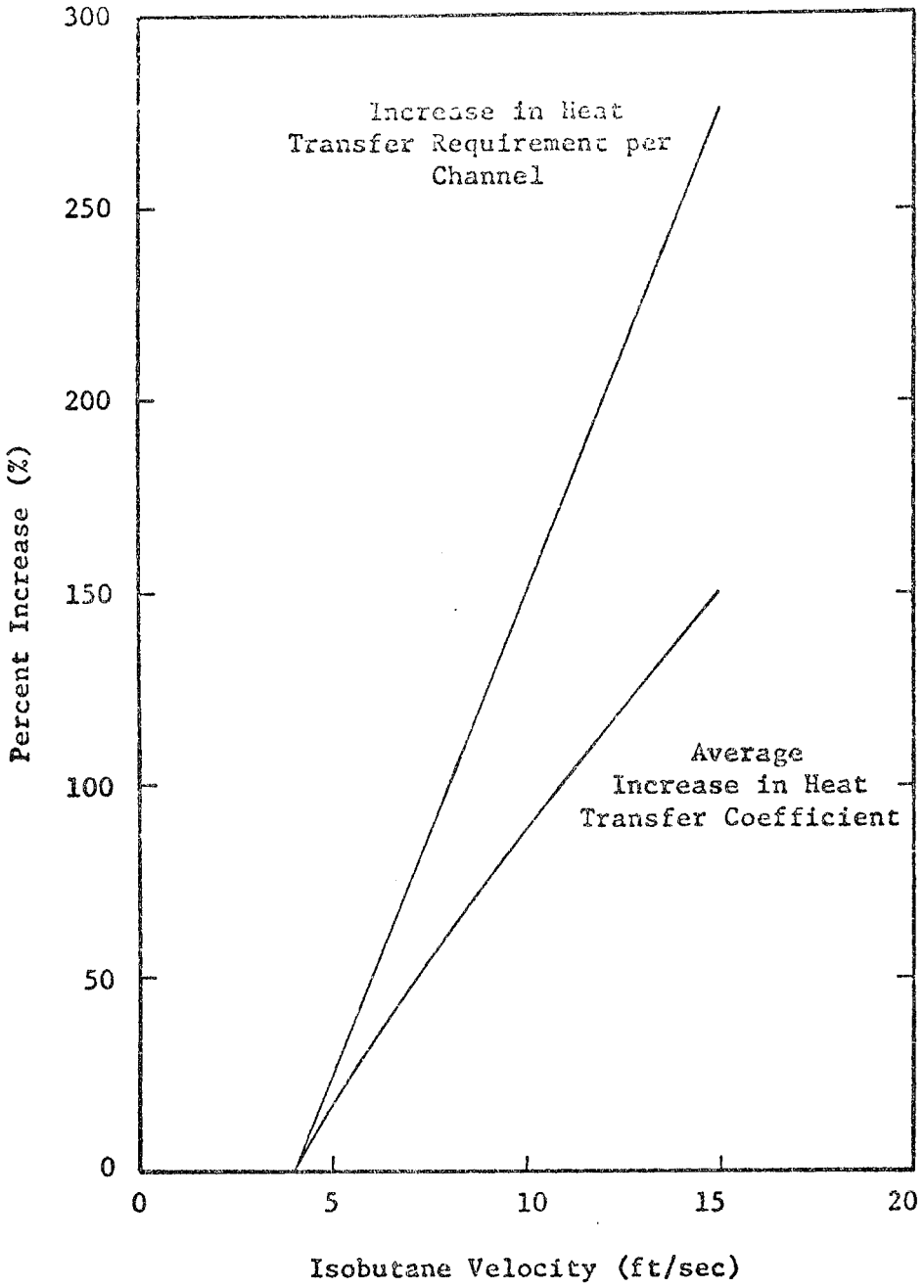

Figure 17 Effect of Isobutane Velocity on Heat Transfer Requirements per Channel and Heat Transfer Coefficient

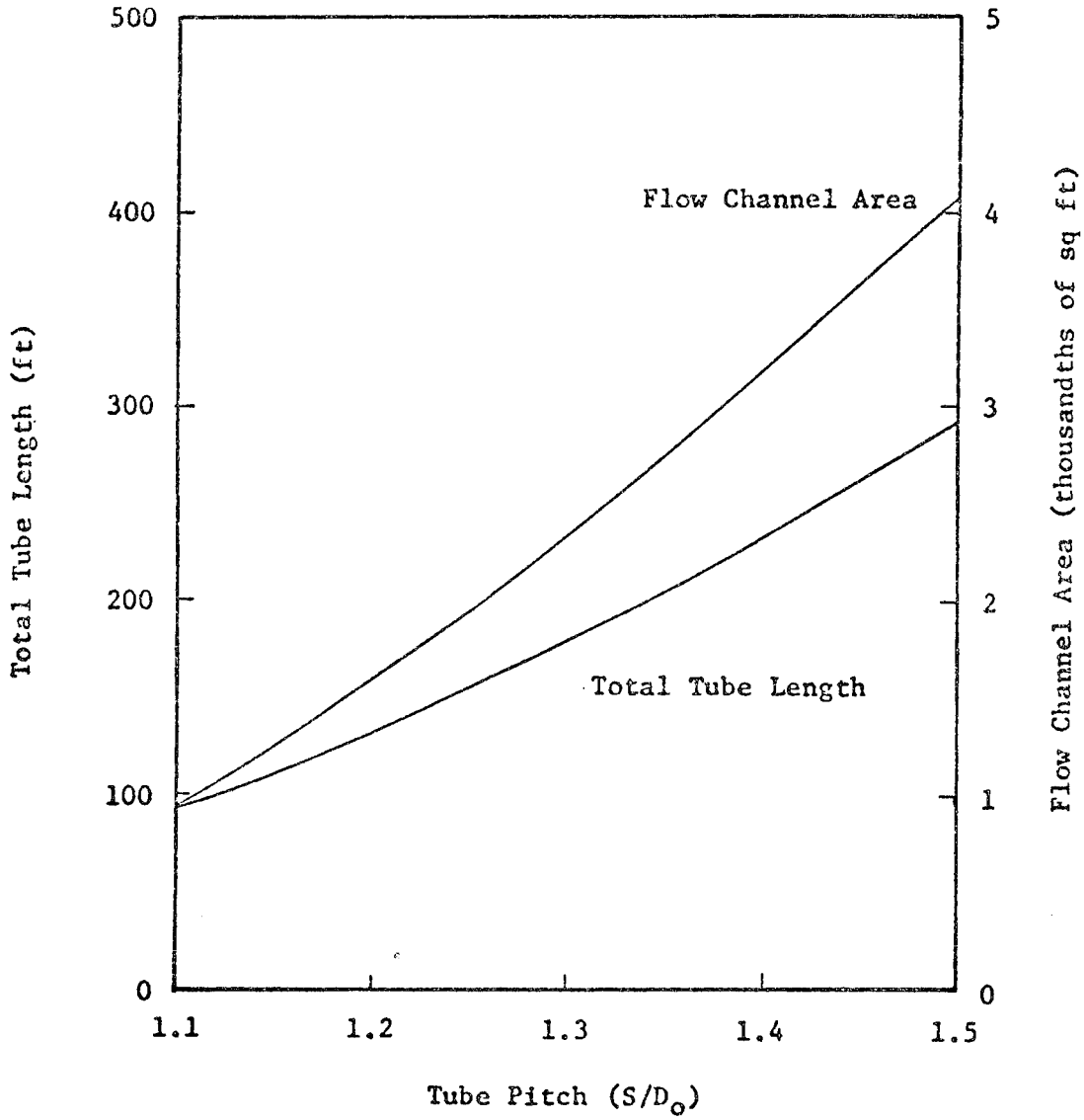

Figure 18 The Effect of Tube Pitch on Total Tube Length and Flow Channel Area

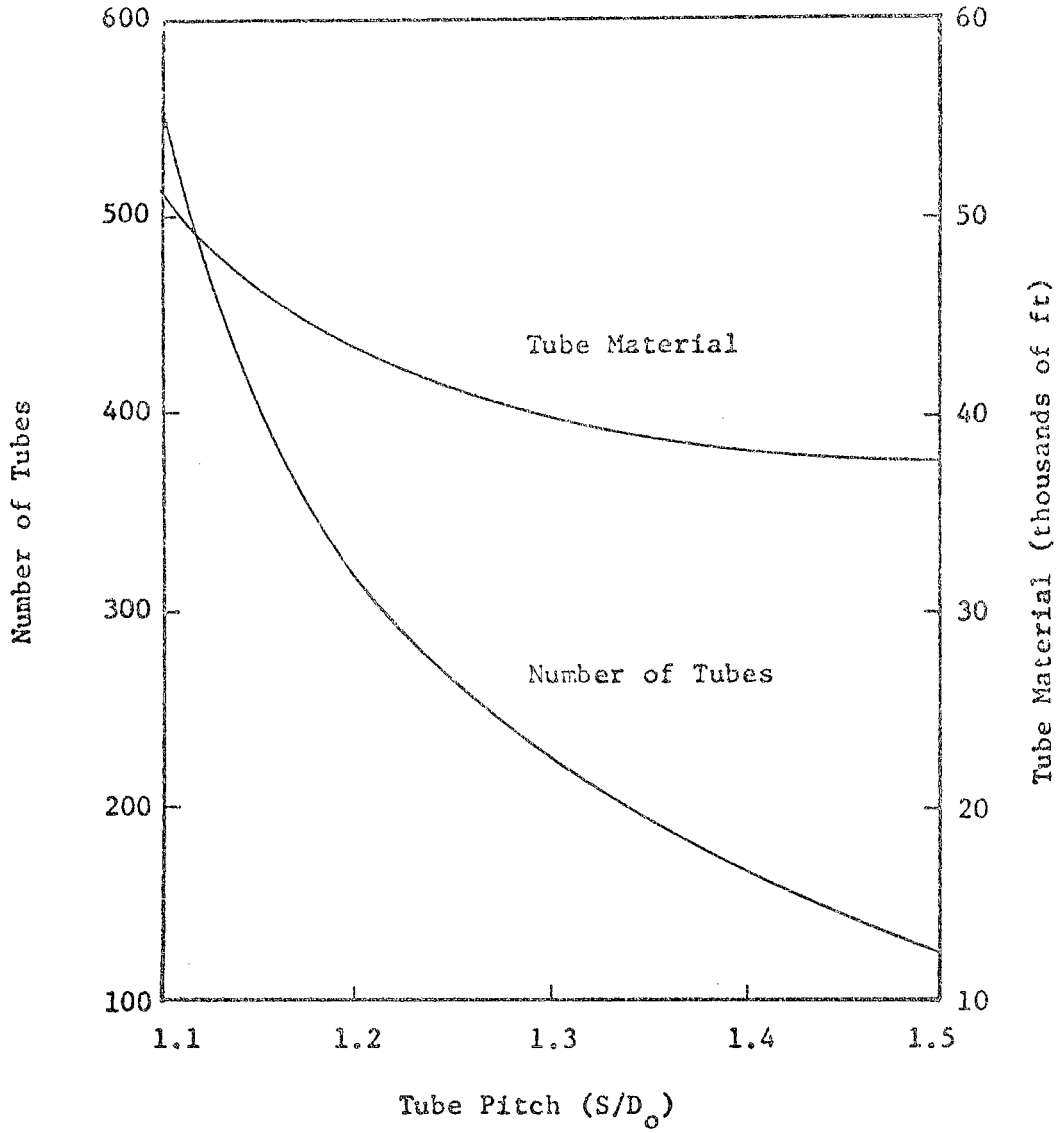

Figure 19 The Effect of Tube Pitch on the Number of Tubes and Tube Material

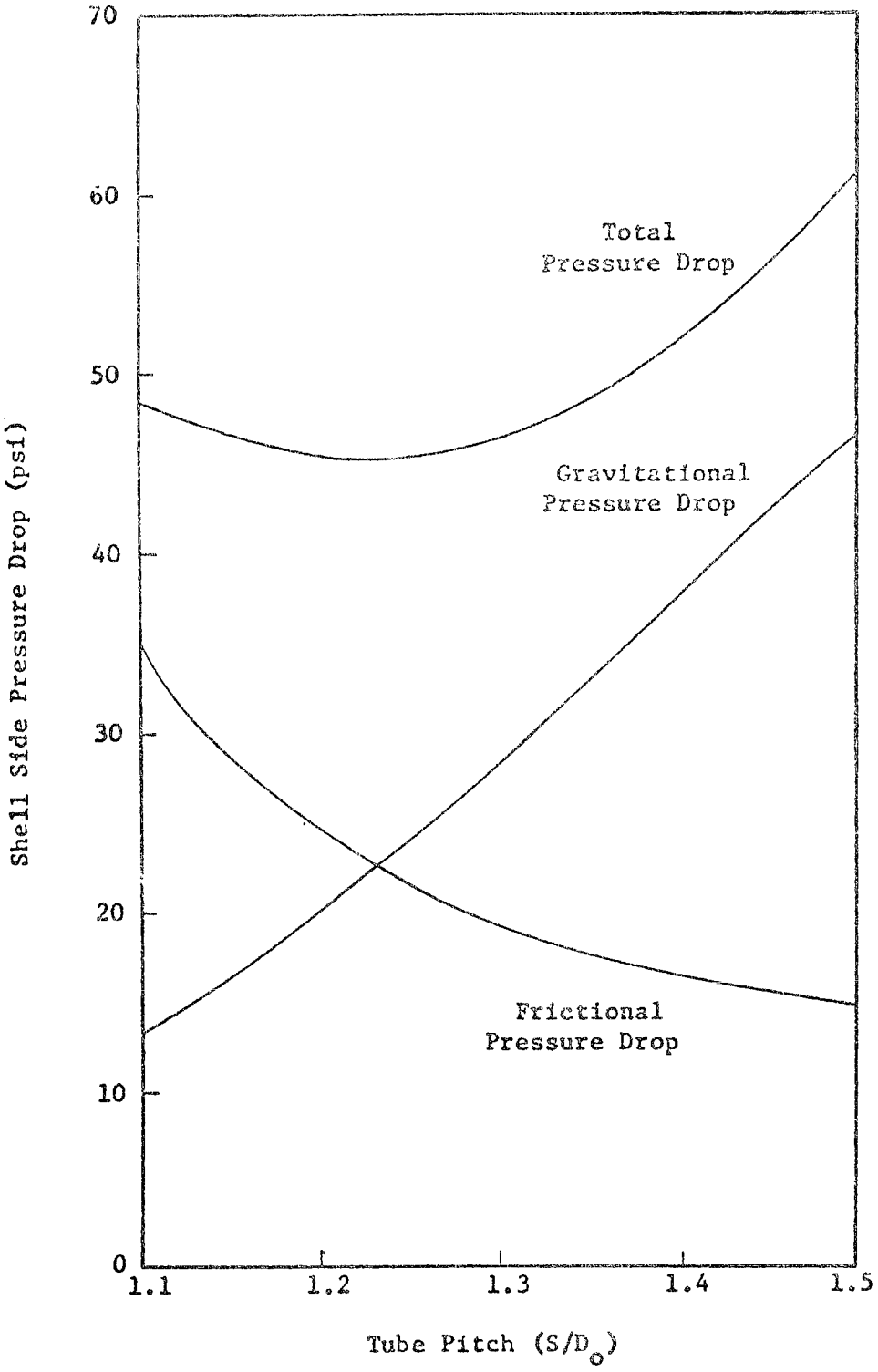

Figure 20 The Effect of Tube Pitch on Shell Side Pressure Drop

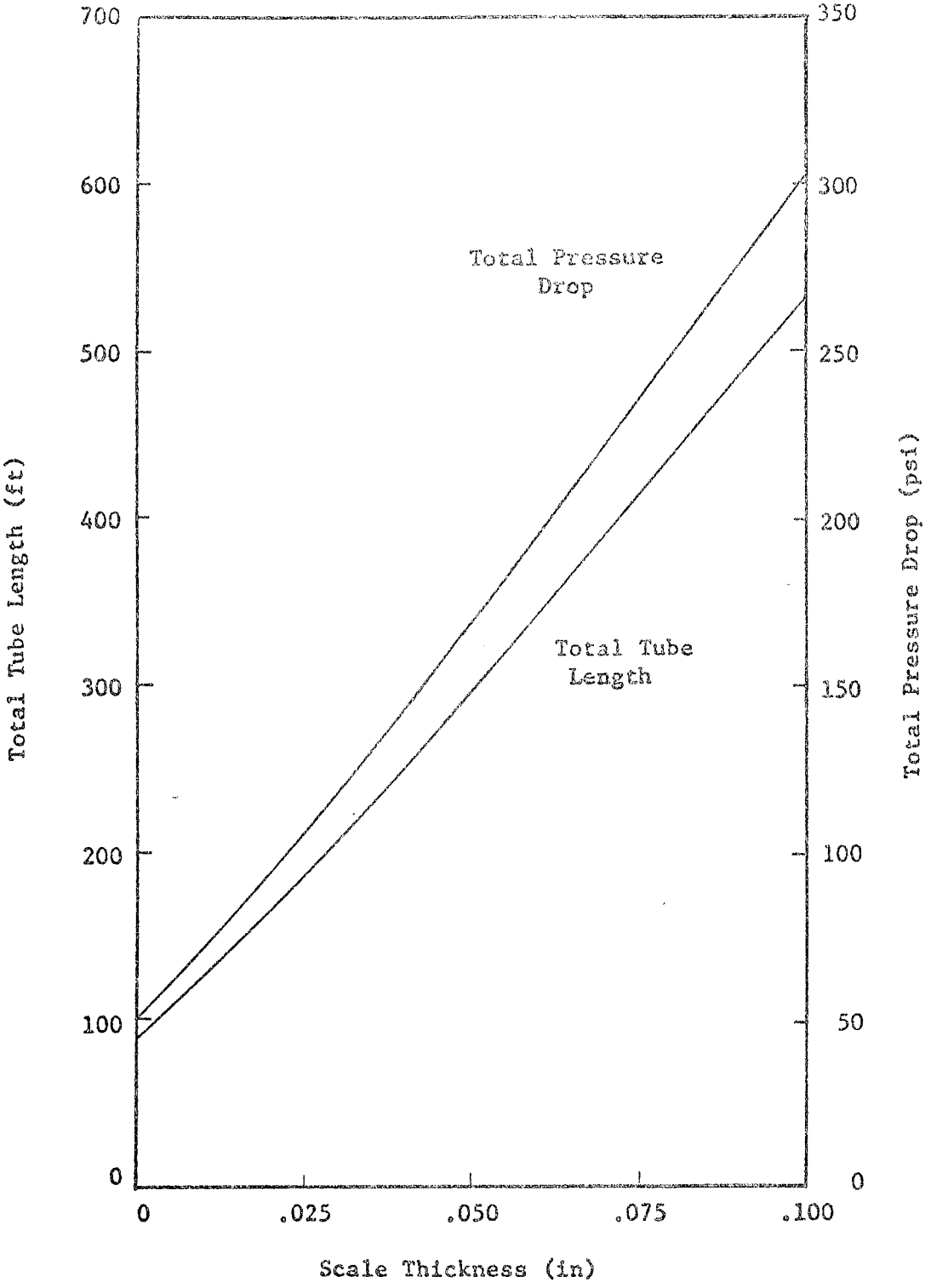

Figure 21 The Effect of Scale Thickness on Total Tube Length and Total Pressure Drop

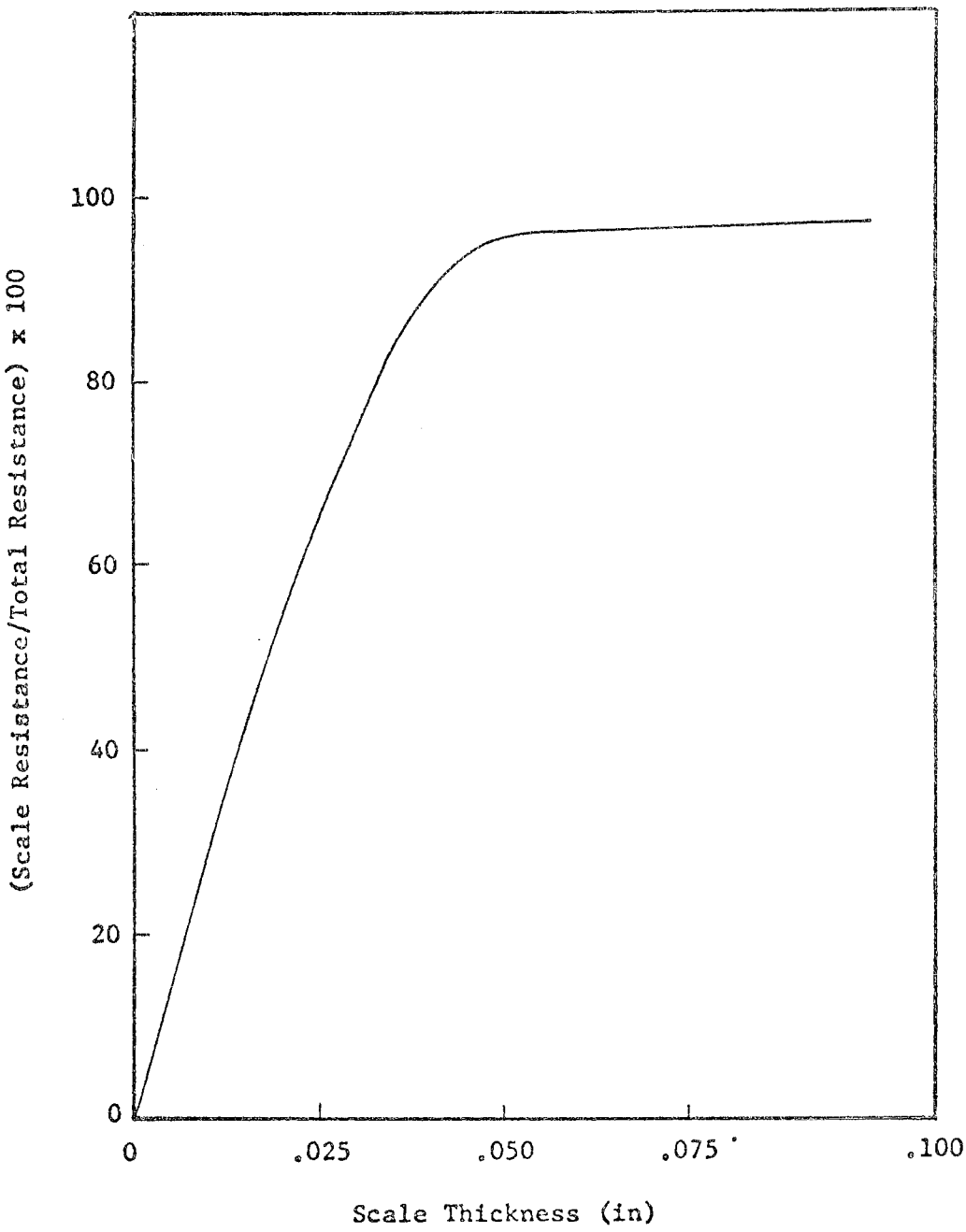

Figure 22 The Relationship Between Scale Resistance and Total Resistance

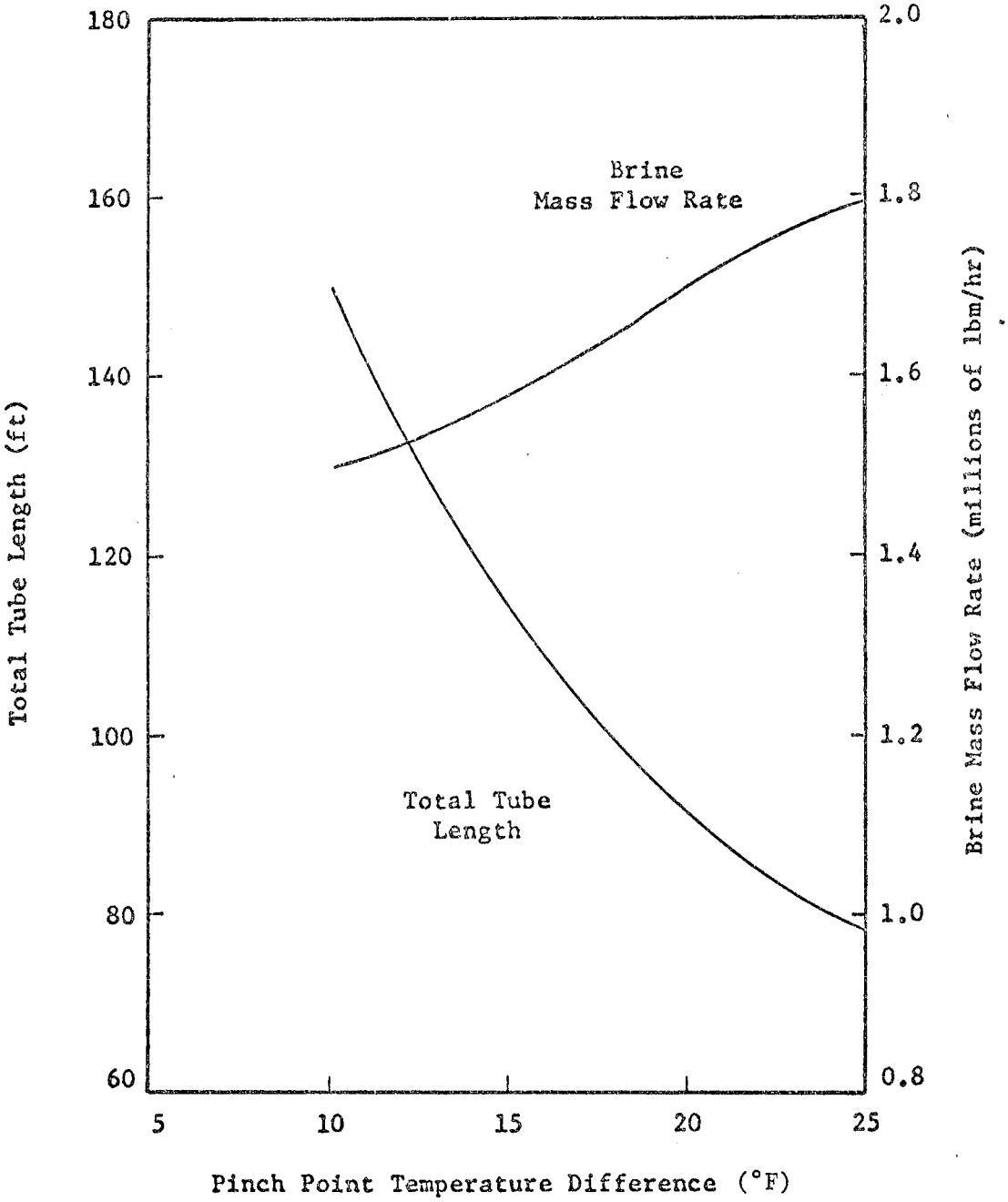

Figure 23 The Effect of Pinch Point Temperature Difference on Total Tube Length and Brine Mass Flow Rate

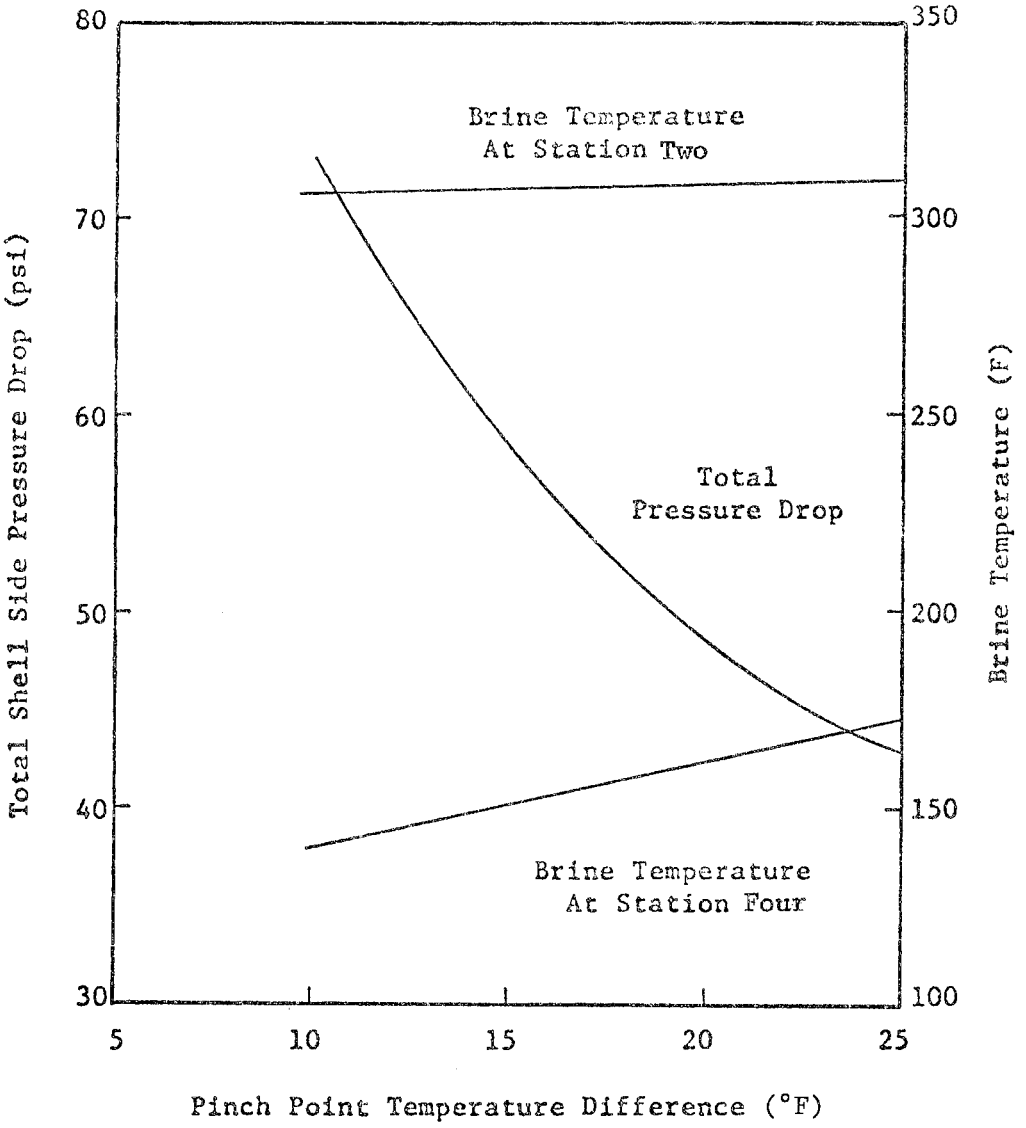

Figure 24 The Effect of Pinch Point Temperature Difference on Shell Side Pressure Drop and Brine Temperature

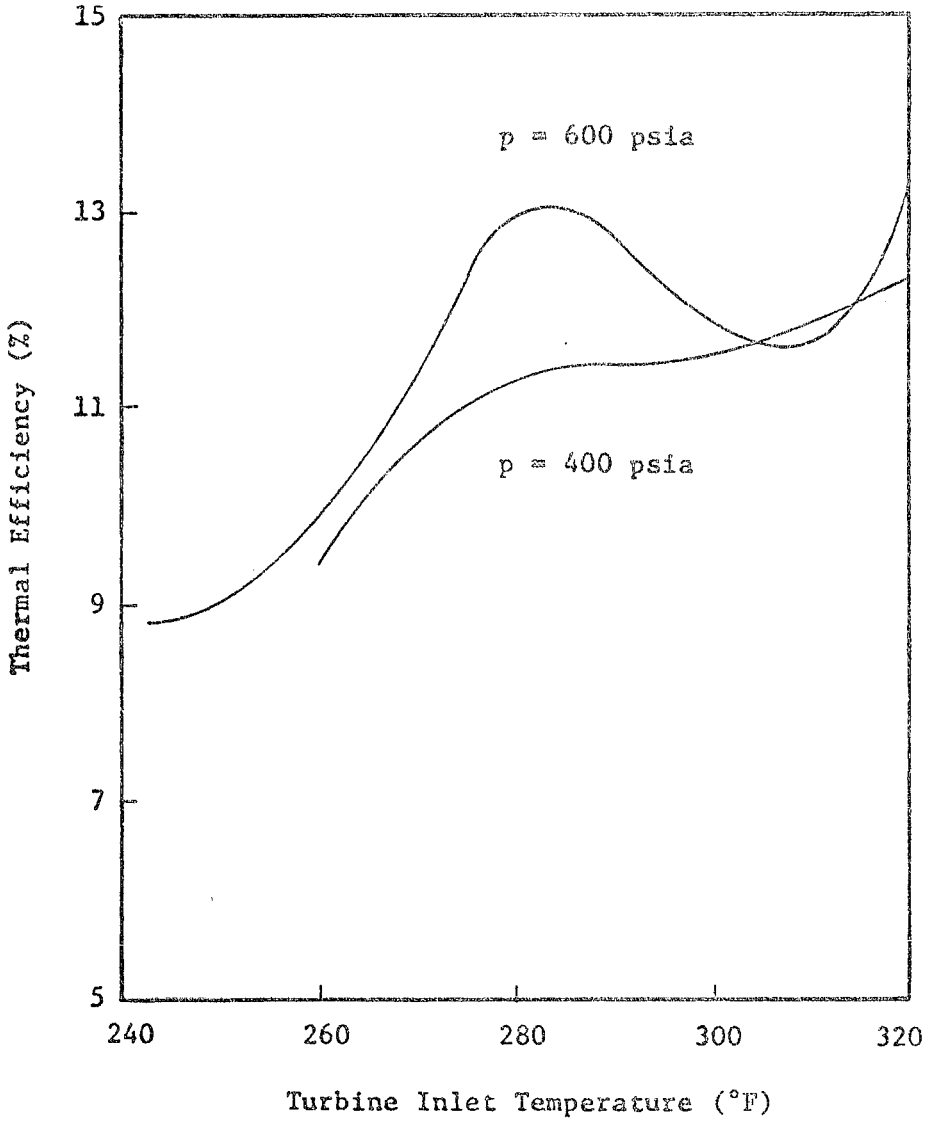

Figure 25 The Effect of Pressure on Thermal Efficiency

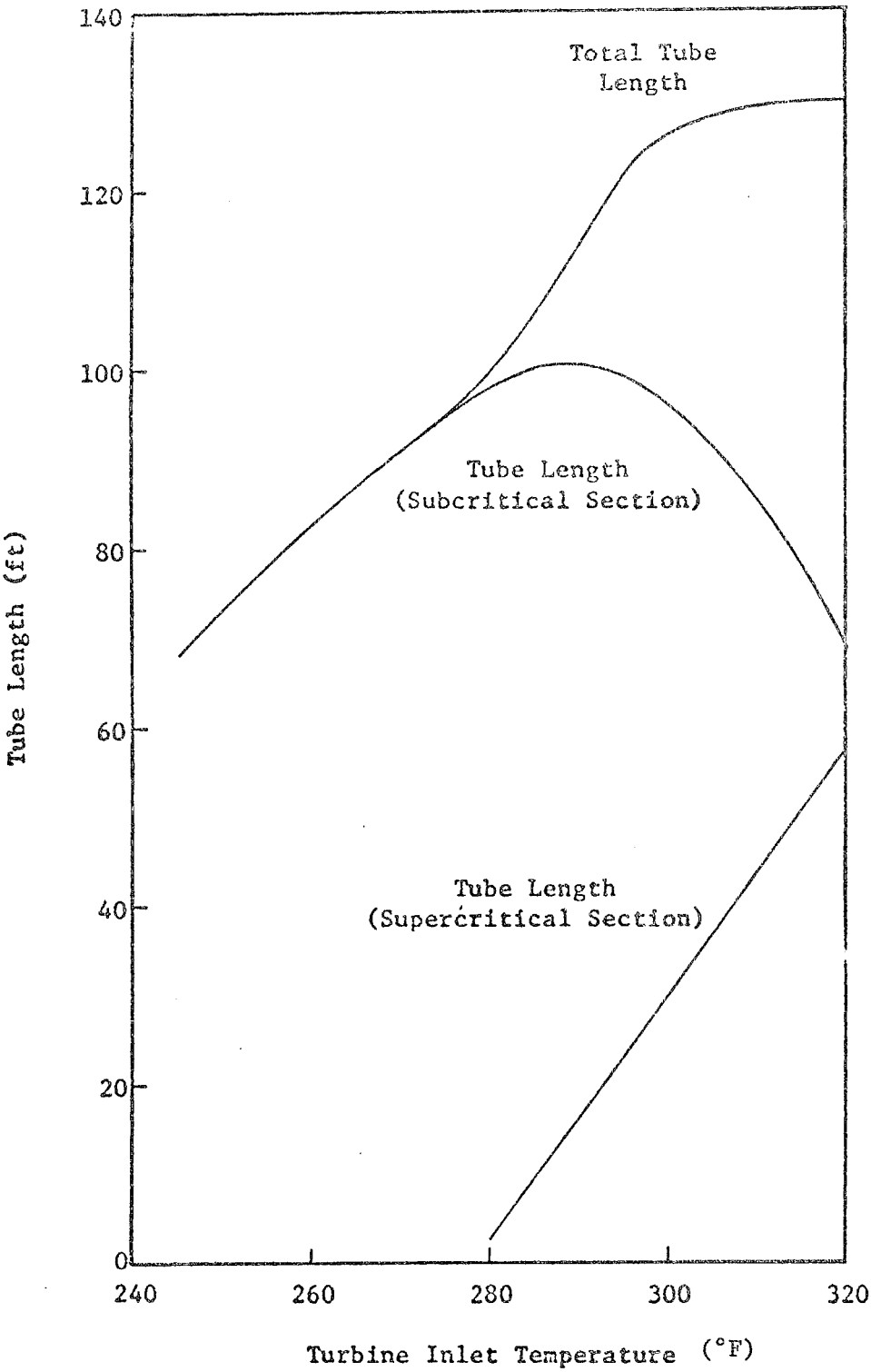

Figure 26 Relationship Between Tube Length and Turbine Inlet Temperature

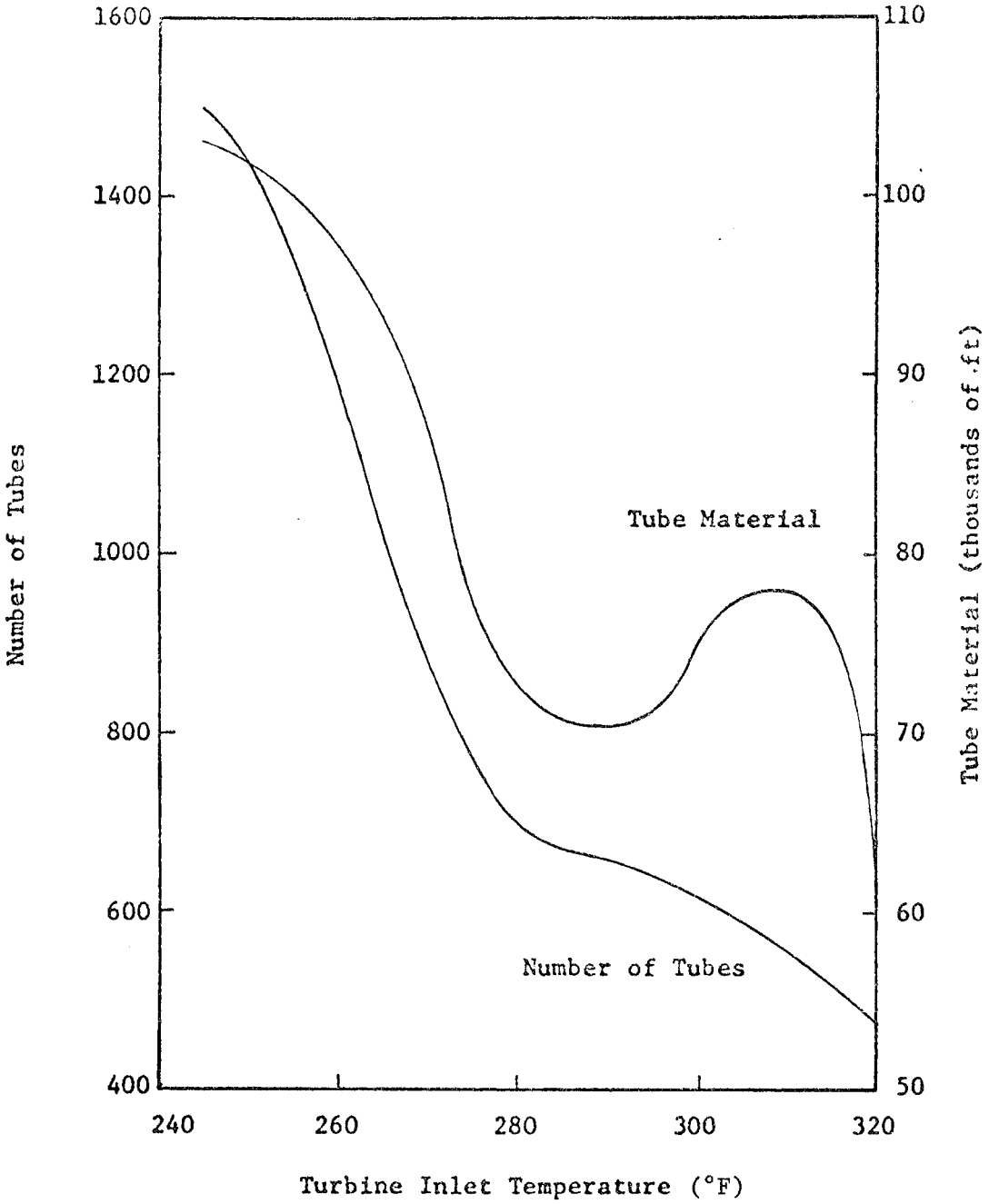

Figure 27 The Effect of Turbine Inlet Temperature on Tube Material and the Number of Tubes

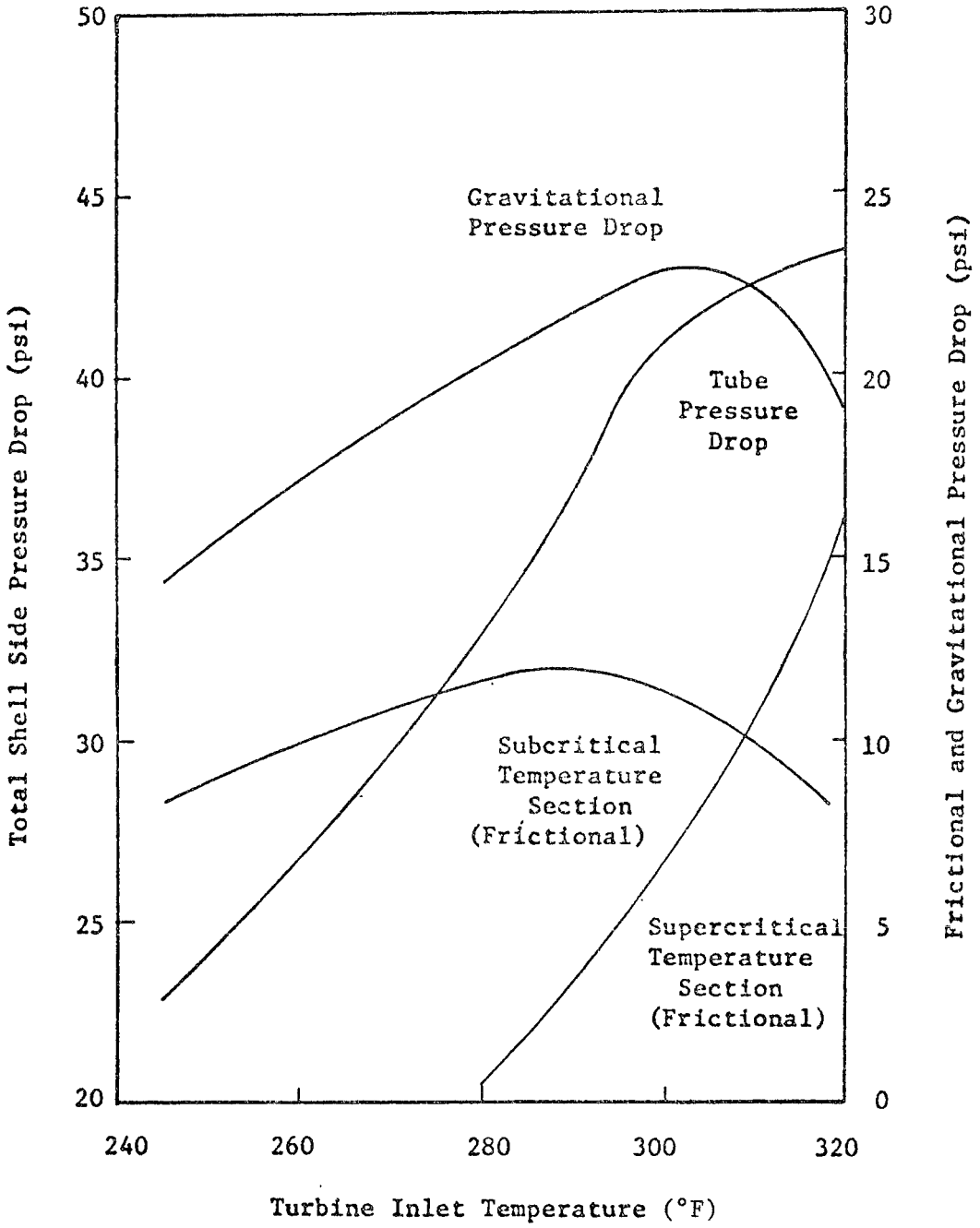

Figure 28 The Effect of Turbine Inlet Temperature on Shell Side Pressure Drop

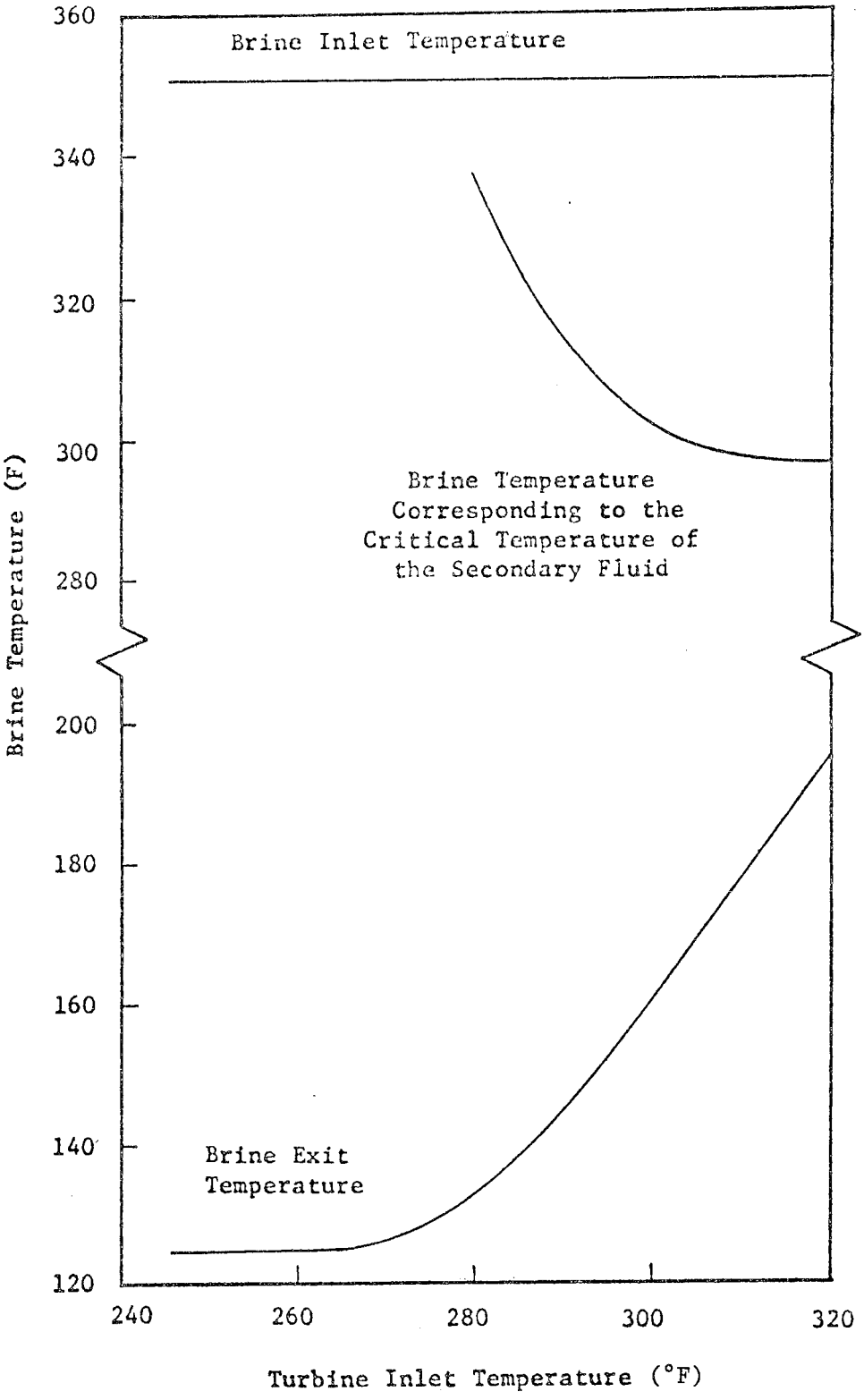

Figure 29 Relationship Between Brine Temperature and Turbine Inlet Temperature

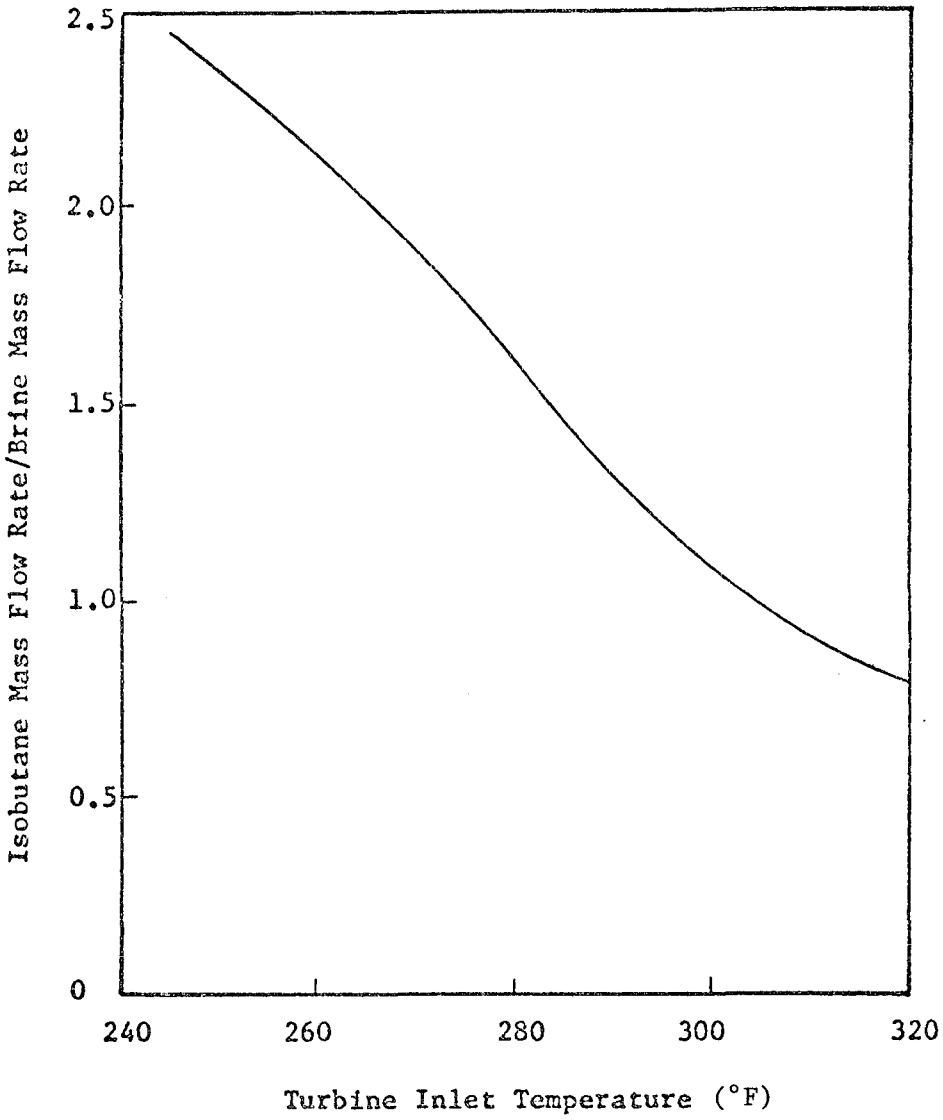

Figure 30 The Effect of Turbine Inlet Temperature on Isobutane and Brine Mass Flow Rates

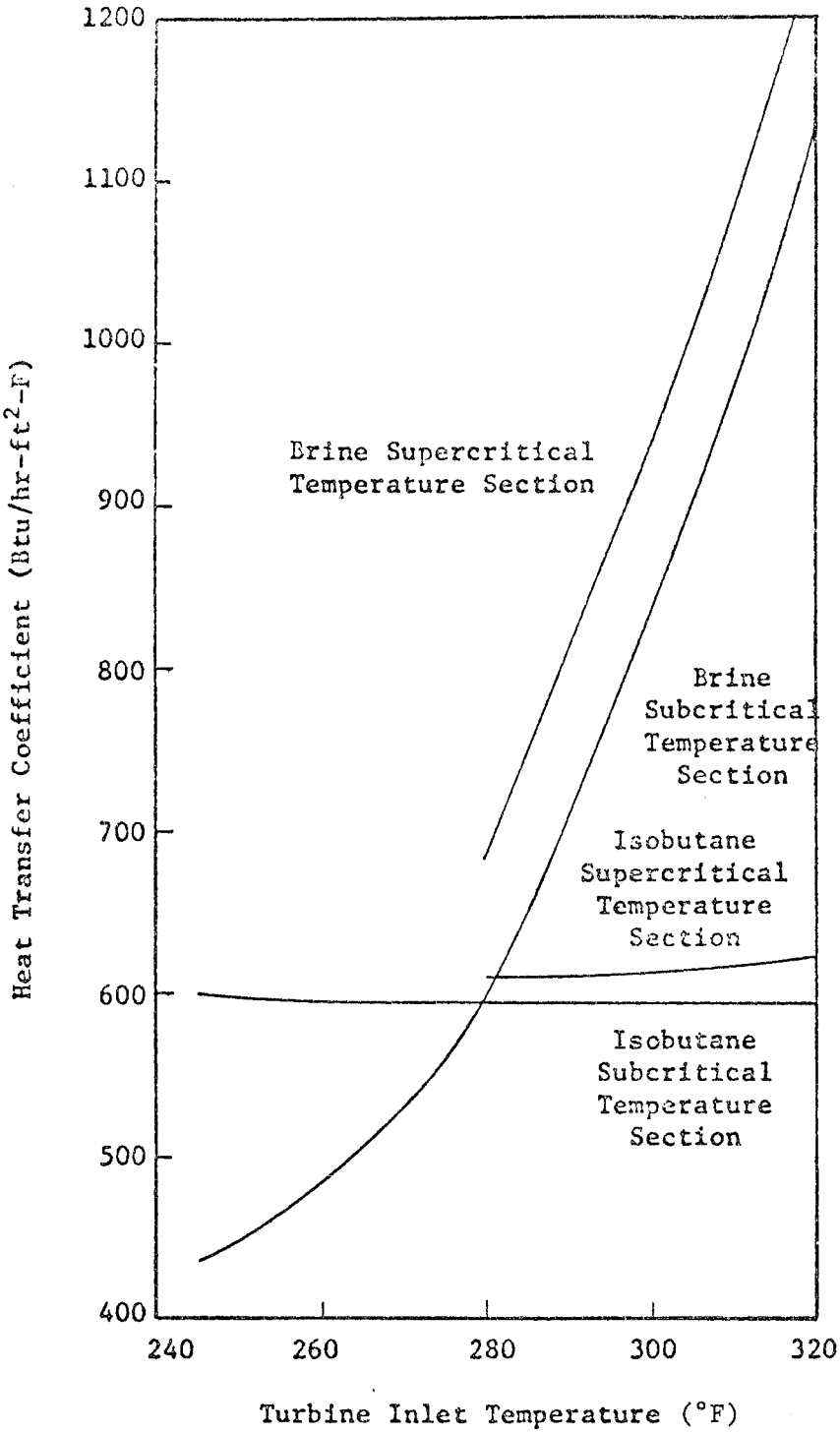

Figure 31 The Effect of Turbine Inlet Temperature on Heat Transfer Coefficients